When Seasonality Constrains Farmer Decisions: Coupled Dynamics of Plant Disease and Clean Seed Use

L. Mailleret [1,2,*], A. Mandal [1], F. Grognard [2], D. Petit [1], F.M. Hilker [3], I. Tankam Chedjou [4], J. Penlap Tamagoua [2], F.M. Hamelin [4]

[1] Université Côte d'Azur, INRAE, ISA, Sophia Antipolis, France
[2] Université Côte d'Azur, Inria, INRAE, CNRS, MACBES, Sophia Antipolis, France
[3] Institute of Mathematics and Institute of Environmental Systems Research, Osnabrück University, Barbarastraße 12, 49076, Osnabrück, Germany
[*]Correspondence: ludovic.mailleret@inrae.fr
[4] IGEPP, INRAE, Institut Agro, Université de Rennes, Rennes, France

ABSTRACT

In seasonal agroecosystems, plant disease dynamics and grower decisions co-evolve, with seasonality constraining when and how control measures are adopted. We develop a semi-discrete behavioural epidemiology framework that couples a metapopulation plant-epidemic model with imitation-based dynamics describing growers' adoption of clean seed practices. In this setting, growers choose, at the time of planting, between using costly disease-free seed and reusing potentially infected farm-saved seed, leading to feedbacks between plant infection and grower behaviour across seasons. We show that clean seed uptake depends critically on the structure of seed-sharing networks. Uptake outcomes range from pure strategies, when clean seed users do not contribute to the farmer seed pool, to mixed strategies, when they do. The transitions between regimes are determined by clean seed cost and disease transmission characteristics. When all growers contribute to the farmer seed pool, clean seeds provide community-wide disease dilution, initiating a free-riding dilemma: growers may avoid clean seed costs while benefiting from the reduced prevalence maintained by others. Counterintuitively, the free-riding phenomenon leads more transmissible diseases to generate higher clean seed uptake, which subsequently improves disease control. In addition, disease suppression is enhanced when clean seed users do not participate in disease dilution, as this prevents the emergence of free-riding. Overall, the effectiveness of seasonal plant disease management is shaped by epidemiological, economic and behavioural factors, including grower decision-making, seed system organization and policy interventions such as subsidies.

1 INTRODUCTION

The imperative of securing global food provision for a rapidly expanding human population is fundamentally constrained by the prevalence of phytopathogenic agents. These biotic stressors cause substantial and persistent reductions in agricultural productivity, with annual estimates of global yield losses across major staple crops frequently ranging from 10% to over 40% [1]. Such reduction in primary productivity undermines the economic viability of production systems and introduces volatility into regional and international food supply networks [2]. Consequently, the development of robust, long-term strategies for the management of crop epidemics is a fundamental prerequisite for achieving sustainable development goals.

While traditional plant pathology has largely focused on the biological mechanisms of pathogen infection and transmission, recent advancements in behavioural epidemiology – originally developed to study human infectious disease [3] – demonstrate that the efficacy of disease control is critically shaped by human decision-making [4,5]. In human systems, individual responses such as vaccination uptake, social distancing, or treatment adherence are influenced by perceived risks, social norms, and economic incentives, and in turn feed back into transmission

dynamics[5–9]. This bidirectional coupling has been critical for understanding outbreaks such as COVID-19 pandemic, where voluntary compliance and risk perception strongly influenced epidemic trajectories[10]. In contrast to human health decision-making, agricultural grower decisions are largely driven by bioeconomic considerations. Disease and pest management choices are often framed as a "game of strategy", where individual control actions are weighed against economic returns and perceived risks[11,12]. Consequently, understanding this socio-epidemiological feedback is critical for developing effective plant disease control strategies[13].

In this context, it has been demonstrated that when plant disease control measures, such as adopting resistant varieties or clean seeds, are voluntary, individual incentives might fail to align with population-level benefits, resulting in suboptimal uptake and persistent disease[14]. Similar dynamics arise in pest management, where strategic interactions among farmers in the adoption of Bt crops can result in collective-action failures and the breakdown of resistance management[11]. Behavioural models further highlight that the success of disease control campaigns depends critically on grower responses to policy interventions, risk communication, and local disease prevalence[15]. In systems involving the movement of planting material, such as cassava in Zambia, grower behaviour in sourcing and exchanging seeds directly determines the spatial trajectory of epidemics[16]. Moreover, agent-based and game-theoretic approaches demonstrate that coordinated action and cooperative behaviour among growers can significantly enhance disease suppression, although such outcomes are highly sensitive to participation thresholds and incentive structures[17,18].

A defining characteristic of many agricultural systems is their intrinsic seasonality, characterized by alternating cropping and off-season periods[19]. Within a growing season, disease transmission is characterized by horizontal spread, while between seasons, the pathogen must survive the host-free window[20]. For many economically significant diseases — such as seed-borne fungal infections in cereals or viruses in clonally propagated crops — the primary reservoir is the planting material itself[21]. This mechanism enables vertical transmission, directly linking pathogen inoculum between successive cropping seasons and determining the initial infection pressure at the onset of each new cycle. This cyclic structure of agricultural landscapes imposes fundamental constraints on disease control. Unlike continuous disease control methods (e.g., pesticide application throughout the growing season), many baseline control strategies are seasonal and must be enacted at discrete time points, typically prior to planting[22]. Decisions regarding crop type selection, varietal resistance, crop rotation, and seed sourcing are fixed for the duration of the season and cannot be readily adjusted in response to unfolding epidemic conditions[23]. While recent frameworks have begun to integrate adaptive grower behaviour into plant disease modelling[13,15,24,25], they seldom account for the inherently seasonal and intermittent nature of agricultural decision-making[11,17].

In a seasonal context, growers' decisions regarding seed sourcing play a central role in shaping disease dynamics across cycles. Growers must navigate trade-offs between several contrasting strategies. For example, growers may purchase certified, disease-free clean seeds (CS) to reliably suppress vertical transmission[26,27]. Similarly, they may opt for varieties bred for genetic resistance to specific pathogens[28]. While these strategies significantly lower infection rates, they often incur substantial upfront costs or potential yield trade-offs compared to traditional local varieties. Alternatively, growers may use inexpensive farm-saved seeds (farmer seeds, FS) obtained from previous harvests or shared seed pools[29]. Such a practice, however, might entail inter-seasonal pathogen carry-over, embedding past prevalence into future epidemic risk.

The practical consequences of these individual choices are evident across global agricultural systems. For instan-

ce, in potato cultivation, reliance on uncertified, farm-retained tubers often leads to seed degeneration, where viral loads accumulate across successive generations, severely impacting yields[30]. Similarly, in smallholder bean farming, the recycling of infected seeds serves as a primary reservoir for bacterial blights, allowing the pathogen to persist within the community[31]. While a substantial body of work demonstrated that access to certified clean planting material can significantly reduce initial infection pressure and delay epidemic progression, adoption of such control measures remain limited[13,32]. Context-specific models that capture the delayed nature of preventive strategies – where the decision to invest in clean seed today shapes the epidemiological landscape of the upcoming cropping season – may help explain the gap between theoretically effective control measures and their practical uptake in the field. Advancing long-term prediction and management of seasonal plant diseases therefore requires quantitative frameworks that explicitly couple continuous-time epidemiological processes with discrete-time behavioural adaptation — an approach that remains largely unexplored in plant pathology.

In this paper, we develop a semi-discrete behavioural epidemiology model to investigate coupled plant disease dynamics and grower behaviour in seasonal agricultural systems. We consider the dynamics of plant disease in interaction with the adoption dynamics of clean seed by growers, i.e. the cropping of plants from seeds or other germplasms certified as disease-free. More specifically we examine how clean seed adoption interacts with plant disease dynamics and diffuses among growers at the scale of an agricultural landscape. Growers choose between two seed-sourcing strategies: certified disease-free clean seeds that come at some cost (C-strategy), and farmer seeds obtained from a local farmer managed seed system sourcing plants in the considered landscape (F-strategy). The latter are assumed cost-free, but they may inherit the disease carried by their mother plants. The framework couples continuous-time intra-seasonal plant-disease dynamics with discrete-time behavioural updates at planting. To describe the heterogeneity of grower strategies over the landscape, we embed the epidemic dynamics in a metapopulation structure, where each field acts as a distinct epidemiological unit with its own local dynamics and seed-sourcing strategy. Strategy adoption evolves across seasons through payoff-driven imitation dynamics[33], where relative profitability determines grower behaviour at the population level. We consider two types of farmer seed-sharing networks: a selective seed pooling scenario, where F-strategy growers replant only seed from their own harvest, and a landscape seed pooling scenario, where harvests from all growers are mixed and redistributed to F-strategy growers. In both regimes, C-strategy fields are always planted with fresh, disease-free clean seeds. We investigate how adaptive seed-sourcing decisions, shaped by economic returns and mediated by seed system structure, feed back into seasonal disease dynamics to determine the efficacy of clean-seed adoption in controlling landscape-scale epidemics.

2 MODEL

In the context of seasonal agricultural systems that are characterized by annual cycles of planting and harvesting, our model is rooted in semi-discrete plant epidemiology theory[34,35]. We follow this formalism to depict a plant disease spreading during the cropping season within a metapopulation of field-crops (horizontal transmission of the disease, in continuous time), and from one cropping cycle to the next through seeds (vertical disease transmission, in discrete time). Because the decision to use clean seeds is taken at planting and remains unchanged for the whole crop cycle, growers' behaviour adaptation will also be modelled in discrete time, through game theory interactions, on an annual cycle basis.

For reference, all notations are summarized in Table 1.

Plant disease dynamics

The considered agricultural landscape is made up of n fields, each containing N plants of a given type, clean seeds or farmer seeds. Within the k-th cropping cycle, a proportion p_k of fields are planted with clean seeds. Therefore, during that cycle, the landscape corresponds to a metapopulation formed by $p_k n$ fields planted with clean seeds (C-fields) and $(1 - p_k)n$ fields planted with farmer seeds (F-fields).

The model tracks the dynamics of the disease along annual cycles, each of which is of time length T. During cropping cycles of time length $\tau < T$, the number of infected plants in a C-field I_c and the number of infected plants in an F-field I_f are considered. By definition, at the beginning of the k-th cropping cycle ($t = kT$) C-fields are free from disease: $I_c(kT) = 0$. The initial number of diseased plants in F-fields $I_f(kT)$ changes with respect to the scenario considered, but generally depends on the number of infected plants in the landscape and the proportion of C-fields in the previous cropping season (see below).

In-season dynamics of the disease are governed by SI-like equations, with infections originating either from infected plants in the same field, or from infected plants in other fields through a common inoculum pool[36,37], driven by the total number of infected plants in the landscape I_ℓ. At any time $t \in [kT, kT + \tau]$, I_ℓ can be inferred from field disease dynamics and the distribution of C- and F-fields over the landscape in the corresponding cropping cycle, through:

$$I_\ell(t) = (1 - p_k)nI_f(t) + p_k nI_c(t). \tag{1}$$

The k-th in-season disease dynamics in C- and F-fields thus obey the following differential equations, for t in $[kT,\ kT + \tau]$:

$$\begin{aligned} \dot{I_c} &= \beta(N - I_c)I_c + \gamma(N - I_c)((1 - p_k)nI_f + p_k nI_c), \\ \dot{I_f} &= \beta(N - I_f)I_f + \gamma(N - I_f)((1 - p_k)nI_f + p_k nI_c), \end{aligned} \tag{2}$$

with β and γ the within- and between-field infection rates, respectively.

At landscape scale, disease dynamics are assessed through the number of infected plants I_ℓ, which is the most relevant measure of disease impact for stakeholders.

Clean seed uptake

Hereafter, we assume a direct correspondence between a field and a crop grower; therefore, the proportion of growers using a given seed strategy is equal to the proportion of fields planted with that seed type in the landscape.

The proportion of growers opting for using clean seeds in their field during the $(k + 1)$-th cropping cycle is noted p_{k+1}. This proportion is determined by the respective performances of the clean seed versus farmer seed strategies during the previous cropping cycle k. Performances of the strategies are evaluated at field scale, through the payoff they yield during a given cropping cycle.

The payoff from the clean seed strategy (C-strategy) during cropping cycle k, $\Pi_{c,k}$, is computed as the profit earned from the sale of mature plant harvest (both free from disease and infected), minus the cost of clean seeds:

$$\Pi_{c,k} = g(N - I_{c,k}) + (1 - \delta)gI_{c,k} - cN, \tag{3}$$

using $I_{c,k} = I_c(kT + \tau)$ as a shorthand notation for the number of infected plants I_c at the end of the k-th crop cycle. Parameter g stands for the profit from a healthy plant, δ the percentage of profit loss on a plant due to the disease and c the unit cost of clean seeds.

For the farmer seed strategy (F-strategy), the payoff only depends on plant sales, because farmer seeds are assumed to be shared freely among growers [38]:

$$\Pi_{f,k} = g(N - I_{f,k}) + (1 - \delta)gI_{f,k}, \tag{4}$$

with the notation $I_{f,k} = I_f(kT + \tau)$.

The proportion of growers using clean seed in a given cropping cycle is then determined from an adapted imitation dynamics equation, stemming from game theory. In its simplest form, the imitation dynamics equation is a discrete-time analogue to the continuous-time replicator dynamics [33]. It states that the probability to use a strategy at a given time step is equal to that probability in the previous time step multiplied by the ratio of payoff of that strategy to the mean payoff in the population of players. Therefore, if one strategy yields a better (resp. poorer) payoff than the other, its frequency in the population increases (resp. decreases) from one time step to the next.

The adapted imitation dynamics used in the present study further accounts for behavioural conservatism in decision taking [39–41], through a weighted sum of the imitation dynamics equation and of the frequency of the considered strategy in the previous time step. Therefore, the proportion of C-fields in cropping cycle $(k + 1)$ is equal to:

$$p_{k+1} = s\frac{\Pi_{c,k}}{(1 - p_k)\Pi_{f,k} + p_k\Pi_{c,k}}p_k + (1 - s)p_k, \tag{5}$$

with $s \in [0, 1]$ being a 'flexibility' parameter describing how flexible growers are in switching strategies: when $s = 0$, growers are inflexible and never change strategy, while when $s = 1$, they fully comply with classical imitation dynamics.

Seasonal transition

In the present model, between season transmission of the disease is assumed to occur through vertical transmission from mother plants to seeds. By definition, clean seeds break this route; however, the disease can spread through farmer seeds that are shared and planted by the F-strategy growers during the next cropping cycle.

At the beginning of the $(k + 1)$ cropping cycle in C-fields, all plants are free from disease so that:

$$I_c((k + 1)T) = 0. \tag{6}$$

For F-fields, two alternative scenarios are considered depending on how farmer seed pools are constituted for

the next cropping season: the *Selective* and the *Landscape seed pooling* scenarios. In both cases, the probability of infection of a seed in the farmer seed pool in season $(k+1)$ is computed as the probability of plant infection among the fields contributing to the seed pool at the end of season k, multiplied by ν, the probability of disease transmission to seeds.

Selective seed pooling.

In this scenario, farmer seed pools are sourced only from F-fields. The probability a plant is infected in F-fields at the end of cropping cycle k is the number of infected F-field plants in the landscape, $(1-p_k)nI_f(kT+\tau)$, divided by the total number of F-field plants in the landscape, $(1-p_k)nN$. At the beginning of cycle $(k+1)$, each field is planted with N plants, so that each F-field starts with:

$$I_f((k+1)T) = \nu I_{f,k}, \tag{7}$$

infected plants.

Landscape seed pooling.

In this scenario, farmer seed pools are sourced from all fields in the landscape, thereby contributing to disease dilution within the seed pools due to the lower expected disease prevalence in C-fields compared with F-fields. Driven by this disease dilution effect such a seed-sharing network structure, if optimally exploited, can achieve more effective disease suppression and yield higher payoffs relative to the *Selective pooling* case. We further investigate and illustrate these properties later in this study (Fig. 6b,d., Appendix G).

In the *Landscape seed pooling* scenario, the probability a plant is infected in the landscape at the end of cropping cycle k is the total number of infected plants, $(1-p_k)nI_f(kT+\tau) + p_k nI_c(kT+\tau)$, divided by the total number of plants, nN. At the beginning of cycle $(k+1)$ each F-field thus starts with:

$$I_f((k+1)T) = \nu\left((1-p_k)I_{f,k} + p_k I_{c,k}\right) \tag{8}$$

infected plants.

Negligible between-field transmission

In the following, we consider that plant disease epidemics are essentially driven by within-field (plant-to-plant) and season-to-season (plant-to-seed-to-plant) transmissions. We therefore assume that between-field transmission is negligible; this corresponds to $\gamma = 0$ in Equation 2. This situation is relevant in different contexts, as fragmented landscapes in which agricultural plots are fairly isolated from one another, owing to distance (scattered landscape), or to the presence of hedges or other environmental elements that limit field-to-field disease transmission. Other examples include greenhouses and other protected cropping systems, for which the barrier to disease spread is physical. From a plant-disease point of view, several plant pathogens combine seed-borne transmission with short-range local spread and little to no natural dispersal between fields. For example *Xanthomonas campestris pv. campestris*, the causal agent of black rot in crucifers, persists mainly in infected seeds, which serve as the primary survival route between seasons, and spread locally within fields via rain splash or plant contact[42]. Similarly, seed-borne bacterial pathogens, such as *Acidovorax citrulli* responsible for bacterial fruit

Table 1: Model variables and parameters.

Notation	Designation	Unit	Value
State variables			
I_c	number of infected plants in a clean seed field	#plants	-
I_f	number of infected plants in a farmer seed field	#plants	-
I_ℓ	number of infected plants in the landscape: $p_k n I_c + (1-p_k) n I_f$	#plants	-
p_k	proportion of clean seed fields during cropping cycle k	-	-
Payoffs			
$\Pi_{c,k}$	gain of clean seed strategy during cropping cycle k	Currency	-
$\Pi_{f,k}$	gain of farmer seed strategy during cropping cycle k	Currency	-
Parameters			
n	number of fields in the landscape	#fields	100
N	number of plants in a field	#plants	1000
T	year length	days	365
τ	cropping season length	days	180
β	within-field infection rate	#plant^{-1}.day^{-1}	2.2×10^{-5}
γ	between-field infection rate	#plant^{-1}.day^{-1}	0
c	clean seed cost	€	0.3
g	gain from a healthy plant	€	1
δ	percentage of loss on plant gain due to infection	%	60
s	probability of grower behaviour change on seasonal transition	-	1
ν	probability of disease transmission to seeds	-	0.2
ω	within-field infection rate reduction with additional disease control	%	30

blotch, transmit vertically through seeds and locally from plant to plant through water splash and mechanical contact[43].

Summary

The negligible between-field transmission hypothesis brings about several simplifications that allow to maintain a high degree of mathematical tractability and generality in the analyses. The main consequence is that C-fields, which are planted with disease-free planting materials, remain disease-free throughout the cropping cycles ($I_c(t) = 0$ at any time t), which simplifies further other components of the model. These simplifications, detailed in Appendix B, boil down the semi-discrete model study to low-dimensional season-to-season mappings that can be fully analysed in terms of equilibria and their stability (Appendix C and D).

The *Selective seed pooling* scenario is indeed solely determined by a 1-dimensional season-to-season discrete-time model of disease dynamics in F-fields (Equation C.2). The temporal dynamics of clean seed adoption directly follows from these dynamics (Equation B.3). In contrast with F-fields, Landscape scale disease dynamics, however, do depend on the use of clean seed. Indeed from Equation 1, in the $k-$th cropping cycle, the number of infected plants in the landscape is determined by: $I_\ell = (1-p_k) n I_f$.

In the *Landscape seed pooling* scenario, there is an interaction between F-field disease dynamics and clean seed use (Equations B.5 and B.3). In that case, the scenario dynamics are determined by a 2-dimensional season-to-season discrete-time model, which couples F-field disease dynamics and the proportion of growers using clean seeds (Equations D.1). This direct coupling results from the contribution of healthy plant materials by clean-seed users to the farmer seed pools. As previously, landscape scale disease dynamics depends on both F-fields disease dynamics and the distribution of grower strategies, through: $I_\ell = (1-p_k) n I_f$.

In Appendices C and D, we compute the season-to-season model equilibria and analyse their stability as a function of model parameters for the *selective* and *landscape seed pooling* scenarios, respectively. We specifically focus on disease dynamics at the end of cropping seasons ($t = kT + \tau$) for they determine payoffs of the strategies over a cropping cycle (Equations 3 and 4) and define the distribution of grower strategies in the next cycle

(Equation 5). Different cases are possible, which correspond either to the extinction or persistence of clean seed users, depending on clean seed costs and disease characteristics. These different cases are illustrated through bifurcation diagrams, showing asymptotic properties of the model as a function of parameter values. To assess disease dynamics and severity, we use disease prevalence at field and landscape scales, *i.e.* the proportion of infected plants at the relevant scale, rather than actual plant counts. These variables are entirely equivalent, as they simply represent different rescalings (Appendix A).

3 RESULTS

Disease dynamics

Time-plots of the model variables (disease prevalence at C-field, F-field, and landscape scale; proportion of clean-seed users) are first presented in Figure 1 to illustrate the seasonal plant disease model dynamics in the considered scenarios. In what follows, we primarily focus on situations where the disease is able to persist in the long run, *i.e.* when its season-to-season reproduction number[35] (Appendices C, D) is greater than unity:

$$\mathcal{R}_0 = \nu \exp(\beta N \tau) = \nu h > 1. \tag{9}$$

With h the seasonal or horizontal reproductive factor of the disease. This condition defines the Epidemic Threshold (ET); it ensures that the disease is not eliminated over seasons solely due to low transmission capacity, thereby requiring a control method, such as clean seed.

Selective seed pooling scenario

Temporal dynamics of the model in the *Selective seed pooling* scenario are illustrated in Figure 1a-c., along 15 cropping seasons and for a low clean seed cost. Such setting corresponds to a stable full control, i.e. $p = 1$, equilibrium situation with an endemic equilibrium in F-fields (Appendix C). C-fields are protected from the disease thanks to the no between-field transmission hypothesis.

In this scenario, clean seed users do not contribute to the farmer seed pool, and disease dynamics in F-fields are independent of the use of clean seeds (Fig. 1a). Since new crops are grown each season, a new epidemic starts over in F-fields at each cropping cycle, spread throughout the cropping cycle and is transmitted to the next season through the farmer seed pool, which initiate a new epidemic. These yearly epidemics quickly adopt a cyclical pattern, repeating the same trend from year 3 onward.

Because for this simulation, the clean seed cost is low enough (c is such that Condition C.6 is false), the C-strategy always outperforms the F-strategy (Appendix C). Therefore, the proportion of clean seed users gradually increases to finally reach 100% of clean seed users (full control; Fig. 1b). The sigmoid shape of p_k against time is linked to imitation dynamics (Eq. 5): the number of growers switching from the F-strategy to the C-strategy accelerates when the proportion of clean seed users is low, and eventually decelerates when it approaches the equilibrium $p = 1$.

At the landscape scale, disease prevalence dynamics reflect the gradual increase in clean seed adoption (Fig. 1c). Landscape scale epidemics worsen in the first two seasons, achieving a peak at the end of cropping season 2 that reflects the increase in disease severity in F-fields and the low adoption of clean seed by growers at that time. Landscape prevalence then gradually decreases to 0, driven by the clean seed use spreading among growers so

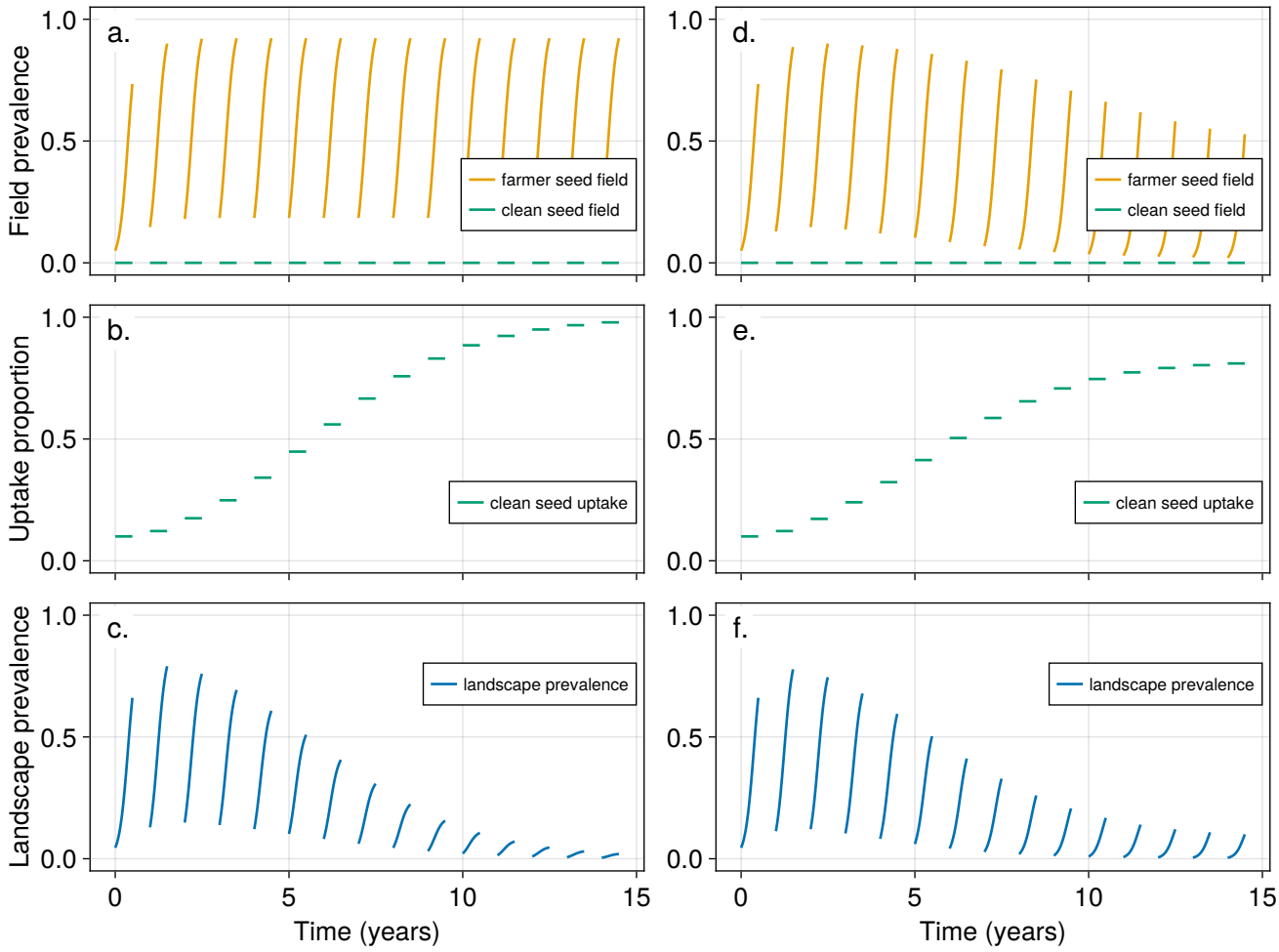

Figure 1: Disease and clean seed adoption dynamics (left column: selective seed pooling, right column: landscape seed pooling). Time plots are represented along 15 cropping seasons for the *selective* and *landscape seed pooling* scenarios. Simulations are not continuous, because no crops are grown between cropping cycles. a, d. C-field and F-field disease prevalence against time. b, e. Proportion of clean seed users against time. c, f. Landscape disease prevalence against time.

that the disease-free C-fields gradually fill the landscape.

Even though F-fields are asymptotically removed from the landscape, the model still keeps tracks of disease dynamics at the F-field level. This is possible because the dynamics are described at the elementary field level and do not simply derive from the metapopulation scale. This is also required, in order to assess what would be the virtual payoff of the F-strategy even in the absence of F-fields. The same observations hold for the C-strategy, should all growers abandon clean seed.

Landscape seed pooling scenario

Temporal dynamics of the model in the *Landscape seed pooling* scenario for a low clean seed cost are presented in Figure 1d-f. The considered parameter set corresponds to a stable mixed control equilibrium situation, i.e. $0 < p^* < 1$, with an endemic equilibrium in F-fields (Appendix C) and partial adoption of clean seed by the grower population. The no between-field transmission hypothesis implies disease-free C-fields, again.

In this scenario, clean seed users contribute to the farmer seed pool, so that the disease dynamics in F-fields and the proportion of clean seed users jointly evolve over time (Fig. 1d-e.). The first cropping cycles dynamics are very similar to the *Selective pooling* scenario, but as the proportion of clean seed users increases, their contribution to the farmer seed pools is more impactful and mitigates the seed pool infection load. The next epidemic in F-

fields then begins with a lower burden, resulting in a lower prevalence at the end of the cropping cycle that helps reduce the seed pool contamination further. As disease prevalence in F-fields declines over cropping cycles, the payoff of the F-strategy increases and ultimately converges to that of the C-strategy. At that point, the distribution of grower strategies settles at $p = p^* < 1$, as the C- and F-strategy yield identical payoffs.

Landscape disease prevalence dynamics capture the gradual increase in clean seed adoption (Fig. 1f); however, in contrast to the *selective pooling* scenario, the disease does not vanish in the long run since a proportion $(1 - p^*) > 0$ of growers stick to the F-strategy. In the following, we refer to this phenomenon as *free-riding*: some growers do not follow the clean-seed control method, but they still benefit from it because others pay for and help mitigate the disease through their participation in the seed pool.

Equilibrium analysis

For the *Selective seed pooling* scenario, the equilibrium proportion of growers using clean seeds exhibits an all-or-nothing outcome, depending on whether the clean seed Uptake Threshold (UT) condition:

$$\frac{c}{\delta g} < \frac{\nu h - 1}{\nu(h-1)}, \tag{10}$$

holds. As shown in Appendix C, when the condition is met, all growers adopt the C-strategy (full control, $p = 1$ at the stable equilibrium, *cf.* Fig. 1a-c.). If it is not, all growers opt for the F-strategy (no control, $p = 0$ at the stable equilibrium).

In the *Landscape seed pooling* scenario, the use of clean seeds exhibits a more graded response than in the *Selective* scenario, while remaining governed by the UT condition (10) (Appendix D). When the condition holds, the use of clean seeds is triggered, but not all growers adhere to it, resulting in a free-riding phenomenon as C- and F-strategists co-exist in a mixed population (mixed control, $p = p_m^* \in (0, 1)$ at the stable equilibrium). If it does not hold, all growers fall back to the F-strategy (no control, $p = 0$ at the stable equilibrium).

Interestingly, the UT condition (10) can be further interpreted in terms of comparison of loss components in the payoffs of the pure F- and pure C- strategies ($p = 0$ and $p = 1$, respectively). Indeed, (10) is equivalent to (Appendix C-D):

$$cN < \delta g I_f^*,$$

with I_f^*, the disease equilibrium level in F-fields when all growers adhere to the F-strategy ($p = 0$). Therefore, the selection between the F- and C- strategies relies on a direct quantitative comparison between the cost of clean seeds for the (pure) C-strategy (cN) and the cost entailed by the disease for the pure F-strategy ($\delta g I_f^*$), with lower (resp. higher) clean seed costs favouring adoption of the C-strategy (resp. F-strategy) by growers.

In what follows, we further illustrate, using 1D bifurcation diagrams, the asymptotic properties of the model in the *Selective* and *Landscape seed pooling* scenarios, as governed by the UT condition (10) and the analyses presented in Appendix C and D. Particular attention is given to the influence of the clean seed cost c when $\mathcal{R}_0 > 1$ (Fig. 2), and to the horizontal reproduction factor h (Fig. 3), as they allow to fully explore the interactions between disease dynamics and grower behaviour.

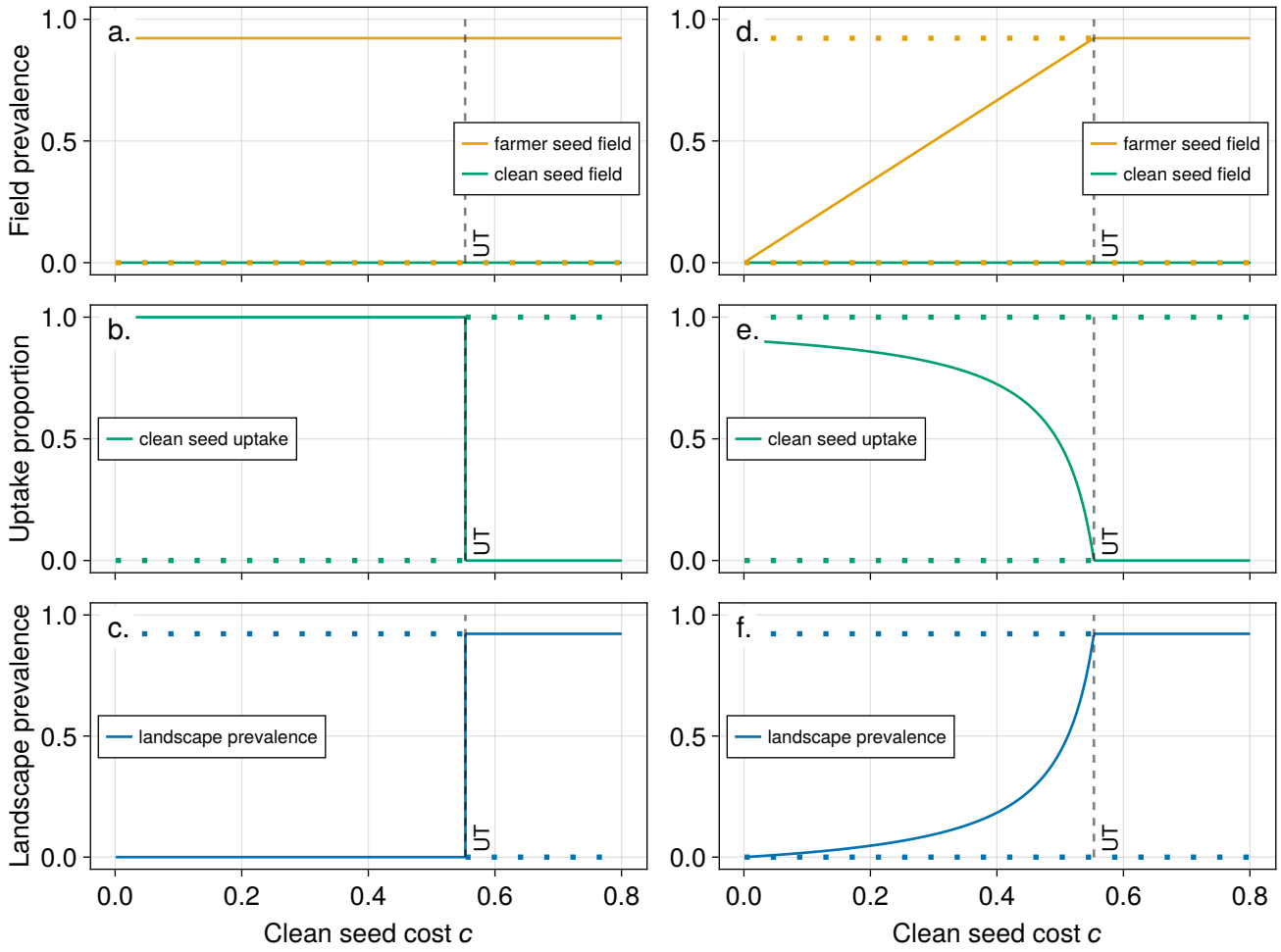

Figure 2: Bifurcation diagram with respect to clean seed cost (left column: selective seed pooling, right column: landscape seed pooling). Equilibria for the *Selective seed pooling* (a-c) and the *Landscape seed pooling* (d-f) scenarios as a function of the clean seed cost c (with $\mathcal{R}_0 > 1$). Stable equilibria are plotted with solid lines, unstable ones with dotted lines. The grey dashed vertical line correspond to a bifurcation threshold (clean seed Uptake Threshold - UT). a, d: C-field and F-field disease prevalence against clean seed cost. b, e: Proportion of clean seed users against clean seed cost. c, f: Landscape disease prevalence against clean seed cost.

Clean seed cost

In the *Selective seed pooling* scenario (Fig. 2, left column), low clean seed costs c lead to adoption of the C-strategy by all growers (Fig. 2b.), thereby implying complete control of the disease over the landscape since it is filled with disease-free C-fields (Fig. 2c.). When clean seed costs are too high and exceed the UT threshold (10), the cost of control cannot match the benefits of disease suppression. The F-strategy is then chosen by all growers (Fig. 2b.). No disease control is actually applied, and the disease remains unchecked at the landscape scale (Fig. 2c.). Because of the particular structure of the *Selective pooling* scenario, disease prevalence in F-fields is unaffected by grower strategies at the landscape scale (Fig. 2a., Appendix C).

In the *Landscape seed pooling* scenario (Fig. 2, right column), low clean seed costs imply heterogenous grower strategies at equilibrium and the free-riding phenomenon (Fig. 2e.). As clean seed costs increase, the proportion of C-strategists declines at an increasing rate until it reaches zero, as the UT condition (10) is crossed. From there, all growers adopt the F-strategy (Fig. 2e.) and the disease is not mitigated at the landscape scale (Fig. 2f.). In the *Landscape pooling* scenario, disease dynamics in F-fields interact with the distribution of grower strategies through the contribution of C-strategists to disease dilution in the farmer seed pool (Appendix D). This relationship is illustrated for low clean seed costs by the negative correlation between disease prevalence in F-fields and

the proportion of C-strategists in the grower population (Fig. 2d-e.), which drives an accelerating rise in disease severity at the landscape scale (Fig. 2f.)

In both situations, the clean seed cost triggering the use of clean seeds by a part or all of the growers is governed by the UT condition (10). From this expression, it can be readily inferred that the threshold is higher when the gain earned from a healthy plant g or the loss caused by the disease δ are high. The threshold is also larger when the disease seasonal transmission factor h, or its probability of transmission to seed ν, are larger. Indeed, the RHS of (10) is both increasing in h and ν through their respective domains of definition.

Disease transmission

Varying the transmission capacities of the disease yields a slightly more complicated picture as the model undergoes two consecutive bifurcations when the horizontal reproduction factor h increases. The first corresponds to $\mathcal{R}_0$ crossing 1, at $h = 1/\nu$, entailing the establishment of the disease (ET). The second corresponds to the clean seed uptake condition (10) becoming true (UT); the latter can be more conveniently interpreted in terms of h as:

$$h > \frac{\delta g - \nu c}{\nu(\delta g - c)}, \tag{11}$$

with $\delta g > c$, otherwise clean seeds are not used for any h, as they would be too costly. In that case, the h-threshold defined in (11) is larger than $\frac{1}{\nu}$.

For both seed-pooling scenarios, when the horizontal reproduction factor h is low, the season-to-season reproduction number of the disease $\mathcal{R}_0$ lies below 1, and the disease dies out from F-fields and the landscape alike (Fig. 3a, c. and d, f.). No control measures are therefore required in that case (Fig. 3b and e). As h increases and crosses $\frac{1}{\nu}$, $\mathcal{R}_0$ overshoots 1 and the disease emerges in F-fields, but not to a degree sufficient to trigger the use of clean seeds (Fig. 3a-b. and d-e.). This leads to the emergence of the disease at the landscape scale too (Fig. 3c. and f.). As h continues to grow, landscape prevalence of the disease increases as well, and peaks at the ET (Fig 3c. and f, Eq. 11). The maximum is reached when h is sufficiently large to produce noticeable epidemics in F-fields, but small enough to not trigger the use of clean seeds by some or all growers in the landscape.

As h grows even further and the epidemic would develop intensely in F-fields, the ET condition (11) becomes satisfied, which triggers the adoption of clean seed in the grower population. In the *Selective seed pooling* scenario, all the growers switch to the C-strategy (Fig. 3b), what brings about complete control of the disease over the landscape (Fig. 3c). In the *Landscape seed pooling* scenario, the interaction between disease and imitation dynamics at the landscape scale tends to balance disease costs in F-fields and clean seed costs in C-fields. The proportion of C-strategists then gradually increases as h does (Fig. 3e), to maintain the balance with a progressively more transmissible disease. The disease prevalence in F-fields becomes independent of h thanks to the contribution of the C-strategy to disease dilution in farmer seed pools (Fig. 3d). As a result, the disease prevalence at the landscape scale gradually decreases with h (Fig. 3f), following the increase in clean seed adoption linked to the higher transmission capacities of the disease.

Very similar results are obtained regarding the influence of ν, the probability of disease transmission to seeds, for both the *Selective* and *Landscape seed pooling* scenarios (not shown).

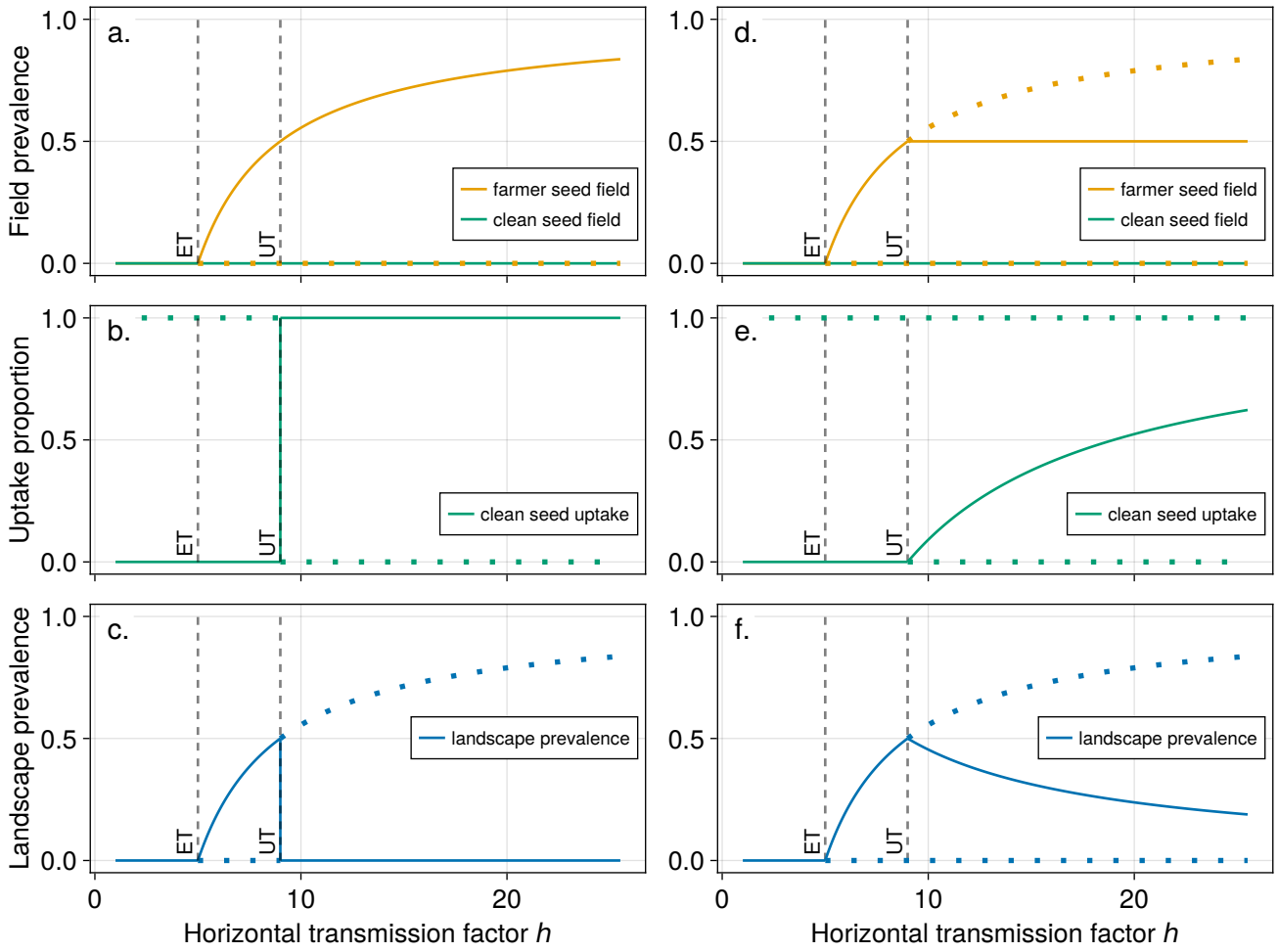

Figure 3: Bifurcation diagram with respect to the horizontal disease transmission factor (left column: selective seed pooling, right column: landscape seed pooling). Equilibria for the *Selective seed pooling* (a-c) and the *Landscape seed pooling* (d-f) scenarios as a function of the horizontal reproduction factor of the diseases $h = e^{\beta N \tau}$. Stable equilibria are plotted with solid lines, unstable ones with dotted lines. The grey dashed vertical lines correspond to bifurcation thresholds (Epidemic Threshold - ET, and clean seed Uptake Threshold - UT). a, d: C-field and F-field disease prevalence against horizontal reproduction factor. b, e: Proportion of clean seed users against horizontal reproduction factor. c, f: Landscape disease prevalence against horizontal reproduction factor.

Disease profile and Clean Seed control

We investigated further in Figures 4 and 7 (Appendix E) how disease characteristics, as captured by transmission parameters h and ν, shape growers' adoption of clean seed and landscape disease prevalence. As already suggested in Figure 3c,f, the least mitigated diseases at the landscape scale are those whose characteristics align with the UT condition (10) (Figs. 4b., 7b.). Disease prevalence is maximal when transmission parameters are large enough to generate a noticeable epidemic, but still low enough to not prompt the use of clean seeds. More transmissible diseases (i.e. with larger $\mathcal{R}_0$) will result in higher adoption levels of clean seed at the landscape scale (Figs. 4a., 7a.), which in turns allow for better or complete mitigation of landscape disease epidemics, depending on the scenario (Figs. 4b., 7b.).

Interestingly, $\mathcal{R}_0$-level curves do not coincide with the level curves of landscape prevalence (Figs. 4b., 7b.). This indicates that the effectiveness of clean seed as a control method varies across disease profiles, due to growers' behavioural adaptation. This is particularly noticeable for moderately transmissible diseases (e.g. $\mathcal{R}_0 = 1.4$ in the Figures). For instance in the *Landscape pooling* scenario, diseases that are more specialized either in transmission to seeds (large ν, small h) or in within season multiplication (large h, small ν) are better suppressed than those with a more balanced profile (Fig. 4b.). The difference is even stronger in the *Selective pooling* scenario,

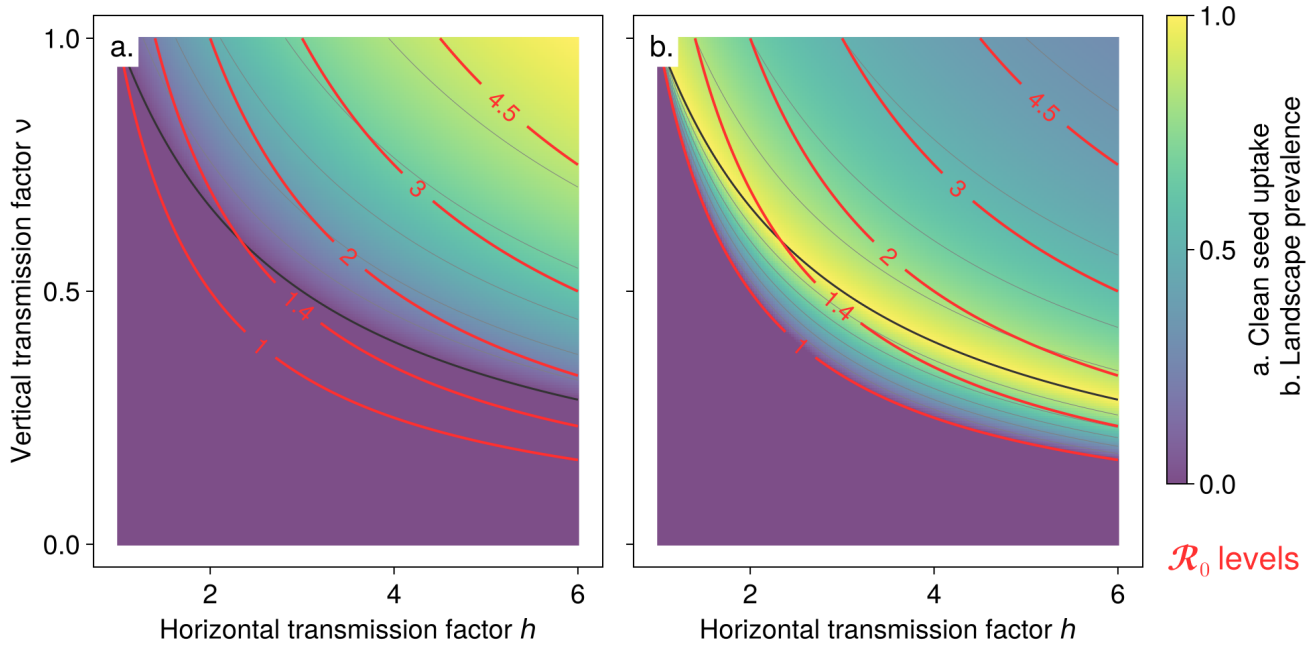

Figure 4: Impact of horizontal and vertical transmission on clean seed uptake and landscape prevalence (Landscape seed pooling). Heatmaps represent the stable equilibrium value of the proportion of CS-fields and the resulting disease landscape prevalence. The thick black line indicates the bifurcation corresponding to clean seed uptake (UT, (10)). Thin grey lines are level curves of the variable associated to the heatmap. Dark red lines indicate constant season-to-season $\mathcal{R}_0$ levels of the disease.

with disease clearance occurring at landscape scale for diseases specialized in transmission to seeds (Fig. 4b.). For diseases with higher transmission capacities (typically $\mathcal{R}_0 \geq 2$) the difference between profiles tends to fade out. This is indeed the case for the *Selective pooling* scenario (Fig. 7b.) where full adoption of clean seed allow clearance for any disease profile in that range. Yet, in the *Landscape pooling scenario*, diseases more specialized towards transmission to seeds are more easily mitigated (Fig. 4b.). These disease profile related effects are more pronounced as the cost of clean seeds c increases. Indeed, the bifurcation curve, which is rooted at $h = 1$ and $\nu = 1$ for any c, attains higher values of ν as c increases (not shown).

Interaction with other disease control methods

Figure 4 suggests unexpected interactions between disease transmission capacities, grower behaviour and realized disease mitigation at the landscape scale in the *Landscape pooling* scenario. An alternative way to examine this question is to explore the consequences of combining clean seed with another control method.

The dynamics presented in Figure 5 illustrate such a situation. The first 15 cropping cycles correspond to a *Landscape seed pooling* scenario as in Figure 1d-f, so that the field prevalence, the proportion of growers adopting clean seeds and the landscape prevalence converge to a mixed-control equilibrium. At the onset of the 16th cropping cycle, an additional control measure that reduces the plant-to-plant infection rate from β to $(1-\omega)\beta$ is adopted by growers. The immediate result is a substantial mitigation of the disease in farmer fields in that cropping cycle (Fig. 5a.). As a consequence, the disease burden in the farmer seed pool is reduced for the next season and the disease in F-fields is further suppressed in the subsequent cropping cycles (Fig. 5a.). In the meantime, since the payoff of the F-strategy increases, it becomes more appealing to growers. As adoption of the F-strategy increases, the uptake of clean seed among growers declines (Fig. 5b.). This in turn diminishes the seed pool disease dilution effect provided by clean seeds, which makes disease prevalence rise again after a few cycles (Fig. 5a.). Ultimately, the proportion of clean seed users settles at a lower equilibrium than before the additional con-

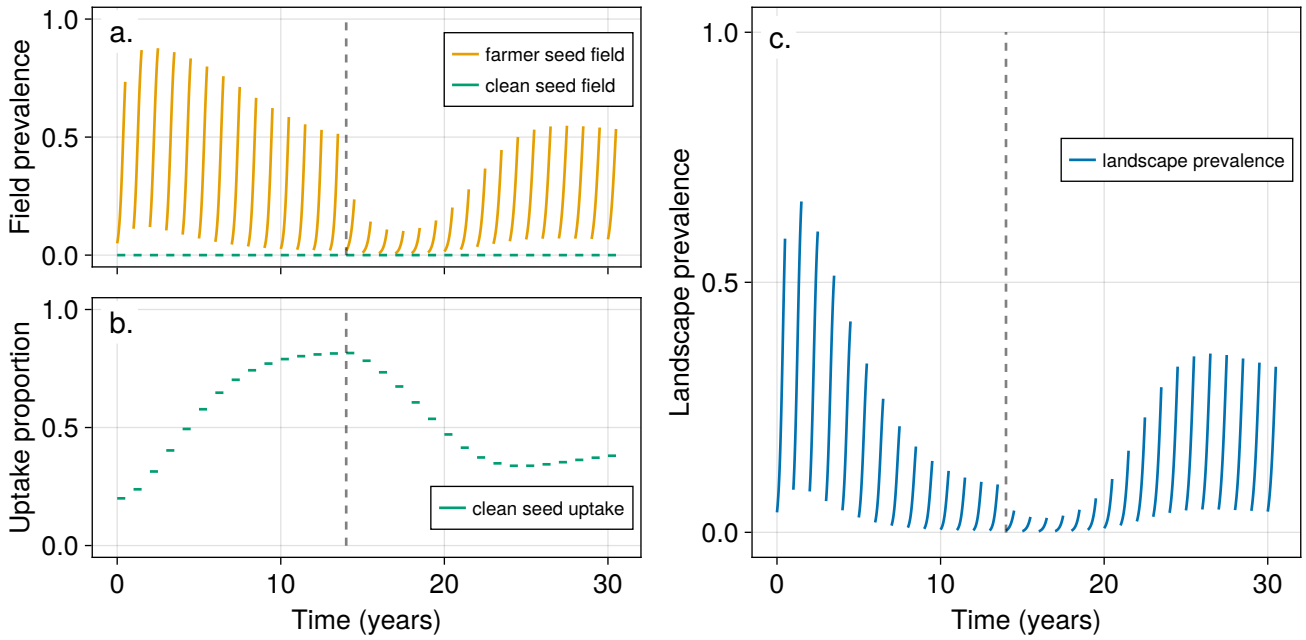

Figure 5: Disease and clean seed users dynamics before and after the triggering of an additional disease control method (Landscape seed pooling). Time plots are represented along 32 cropping seasons for the *Landscape seed pooling* scenario. An additional disease control method switching disease transmission from β to $(1-\omega)\beta$ is activated from season 16 onwards (grey dashed vertical line). a. C-field and F-field disease prevalence against time. b. Proportion of clean seed use against time. c. Landscape disease prevalence against time.

trol method adoption and disease prevalence in F-fields falls back to the mixed-control equilibrium level. At the landscape scale, it results in increased disease prevalence (Fig. 5a-c.). Therefore, at the scale relevant for assessing disease mitigation, the introduction of an additional control method, although effective in the short term, becomes counterproductive in the long term due to the complex feedback loop between disease epidemics and grower behaviour (Fig. 5c.).

This phenomenon is further illustrated in Appendix F, Figure 8, through a bifurcation diagram with the disease control efficacy ω as the bifurcation parameter. It shows that the counterintuitive effect of the additional control method persists across the entire range of ω that permits a mixed-control equilibrium. Although we do not show it here, other additional control methods targeting cycle-to-cycle disease transmission through seeds through a decrease of the parameter ν would yield qualitatively similar counterintuitive results.

Comparison with centralized optimization

Finally, the predictions of the behavioural epidemiology model, where the distribution of clean seed uptake emerges from individual decisions to copy the better performing strategy, are compared with centralized optimization benchmarks, in which a social planner selects the policy that optimizes a global objective. Two global objectives were considered: (i) minimizing disease level at landscape scale (epidemiological optimum), or (ii) maximizing landscape-level payoff (bioeconomic optimum). We show in Appendix G that the epidemiological and bioeconomic optima and the behavioural epidemiology predictions do not necessarily coincide, depending on parameter values and the scenario considered.

In the *Selective seed pooling* scenario, the bioeconomic optimum corresponds to the exact same clean seed uptake rules as predicted by the behavioural epidemiology model (Fig. 6a.). The epidemiological optimum also matches those rules, but only for low clean seed costs, when Equation (10) holds true.

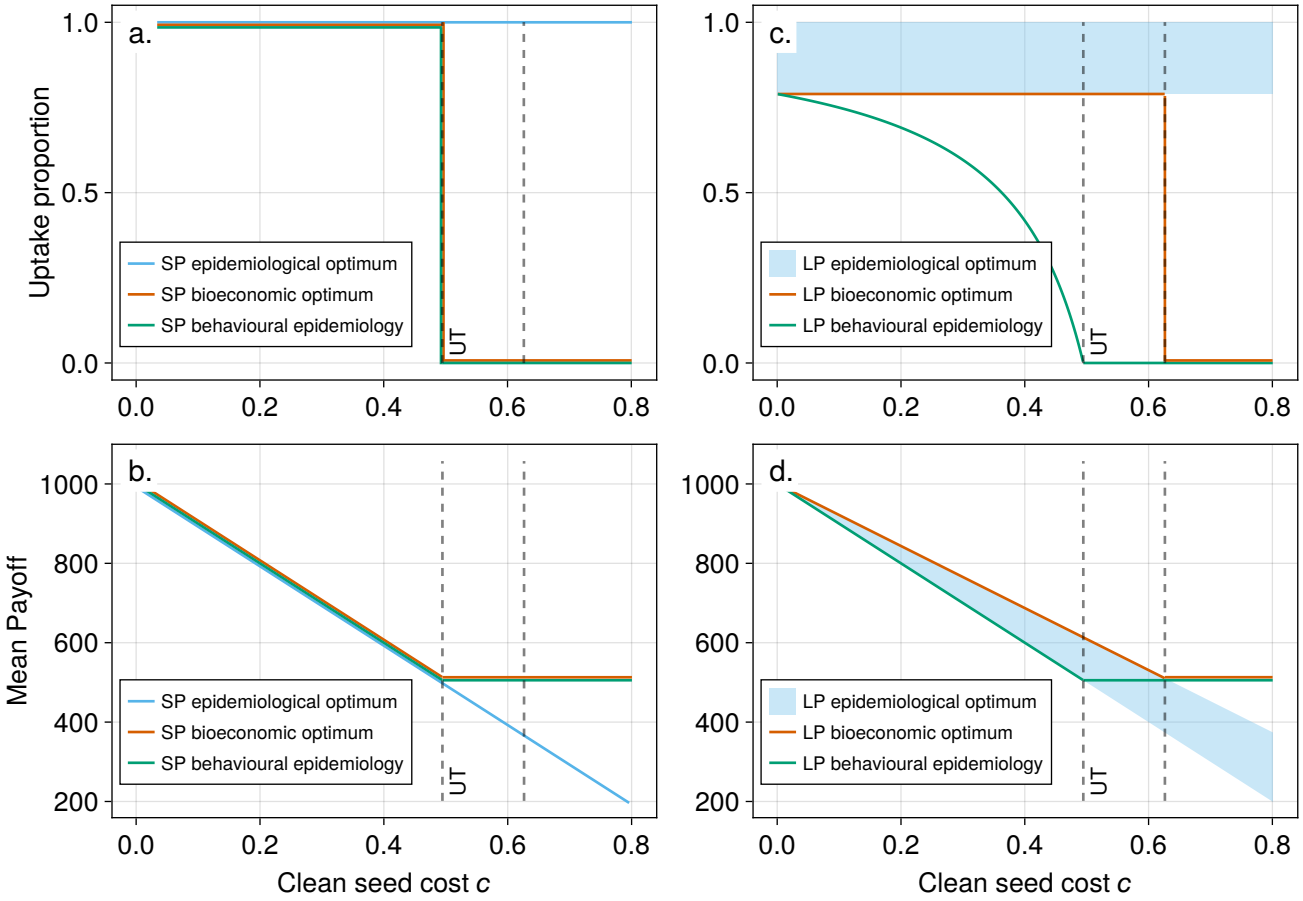

Figure 6: Influence of clean seed cost on optimal clean seed uptake and mean payoffs (left column: selective seed pooling, right column: landscape seed pooling).- Central optimization problems and predictions of the behavioural epidemiology model are displayed. The grey dashed vertical lines correspond to the clean seed Uptake Threshold for the behavioural model (UT) and to the clean seed uptake threshold for the bioeconomic optimum in the *Landscape pooling* scenario (Eq. G.2). SP and LP stand for *Selective pooling* and *Landscape pooling* scenarios, respectively. a, c: Clean seed uptake for the epidemiological (blue) and bioeconomic (brown) optima, and for the behavioural epidemiology model (green). b, d: Mean landscape payoff for the epidemiological (blue) and bioeconomic (brown) optima, and for the behavioural epidemiology model (green). For that specific figure, the parameter β has been reduced by 20% relative to the value in Table 1. Curves that would otherwise overlap have been visually separated to maximize visual clarity.

The analysis of the *Landscape pooling* scenario from the central planner perspective shows direct epidemiological and bioeconomic advantages over the *Selective pooling* scenario, thanks to disease dilution in the seed pool. Indeed, disease can be wiped out from the landscape for any proportion of clean seed users larger than $p_o = 1 - \frac{1}{\mathcal{R}_0} < 1$ (Fig. 6c.). As observed in vaccination epidemiology regarding herd immunity, and in contrast with the *Selective* scenario, it is not required that all growers use clean seeds to eliminate the disease. In addition, bioeconomic optimal clean seed uptake occurs at $p = p_o$ (when Eq. G.2 holds) yielding a larger optimal payoff in the *Landscape* than in the *Selective pooling* scenario (Fig. 6b,d.).

Furthermore, in the *Landscape pooling* scenario, the bioeconomic optimum generally differs from the equilibrium of the behavioural epidemiology model. Indeed, bioeconomic optimal clean seed uptake is strictly larger than p_m^* predicted by behavioural dynamics when $c > 0$. Notably, when c lies between the two thresholds ruling clean seed uptake, the behavioural model predicts growers would give up on clean seeds while the bioeconomic optimum would remain $p = p_o$ (Figure 6c.). In fact, the bioeconomic optimum always imposes a larger clean seed uptake to make the most of disease dilution in the seed pool at the benefit of disease control in F-fields. By doing so, landscape payoff is indeed maximized (Fig. 6d.), the gap with the behaviour model illustrating the "Price of Anarchy" in this system [44]. This maximization occurs however at the expense of fairness: clean seed users, with a payoff $\Pi_c = (g - c)N$, are clearly disadvantaged compared to farmer seed users ($\Pi_f = gN$ in that case), while they

are those who pay for disease control. Only when $c = 0$, or when the bioeconomic optimum is to not use clean seed at all, do both the behavioural epidemiology prediction and the bioeconomic optimum coincide (Fig. 6c,d.).

With respect to disease control, when clean seed cost c is low (Eq. G.2), the bioeconomic optimum is also epidemiologically optimal. But when c is higher, the bioeconomic optimum $p = 0$ is no longer the best from the epidemiological perspective.

In the *Landscape pooling* scenario, predictions of the behavioural epidemiology model diverge from the centralized optimization problems in most cases. Behavioural dynamics would only enable the realization of a bioeconomic optimum, that is also epidemiologically optimal, in the very specific – and arguably unrealistic – case where clean seeds would be free.

4 DISCUSSION

In this study, we developed a semi-discrete metapopulation behavioural epidemiology framework to investigate the coupled dynamics of plant disease and grower behaviour within seasonal agroecosystems. Our approach integrates continuous-time within-season epidemic spread with discrete-time behavioural updates at planting, capturing the annual trade-off between purchasing certified disease-free seeds and reusing inexpensive, yet potentially infected, farmer seeds. Using this framework, we demonstrate that the effectiveness of clean-seed interventions is governed not only by epidemiological and economic factors, but also by the underlying structure of farmer seed sharing networks, particularly the distinction between selective and landscape-scale seed pooling. Based on these alternative seed system structures, decentralized, payoff-driven imitation dynamics can lead either to all-or-nothing regimes (*Selective pooling*), potentially leading to complete disease suppression, or to mixed-control strategies that highlight the emergence of a free-riding phenomenon (*Landscape pooling*).

In the *Selective seed pooling* scenario, the lack of seed exchange between growers following different strategies isolates the epidemiological consequences of individual grower decisions. It results in a binary regime where control is either fully adopted or entirely abandoned, depending on a threshold condition involving clean seed cost and disease transmission characteristics (Fig. 2, 3, left column; Fig. 7). This sensitivity can trigger a catastrophic shift in landscape-scale disease prevalence when the threshold is crossed. In contrast, *Landscape pooling* introduces a shared seed reservoir that functions as a public good; contributions from clean-seed users dilute the inter-seasonal pathogen carryover load, reducing infection pressure across the entire landscape. While this can in principle provide direct epidemiological and economic benefits (Fig. 6b.), it simultaneously erodes the advantages of using clean seed relative to farmer seed. As decentralized decision taking is accounted for through imitation dynamics, a free-riding phenomenon arises for the same threshold condition (Fig. 2, 3, right column; Fig. 4). In such a situation, characterized by the co-existence of both strategies in the grower population, F-strategists benefit from the reduced prevalence maintained by C-strategists, without paying the cost of control. Therefore, seed systems that facilitate collective sharing with decentralized actor-level decision rules are prone to epidemiological and bioeconomic outcomes that are less efficient than the outcomes under centralized coordination (Fig. 6c-d.). Mitigating this risk likely requires policy instruments, such as targeted subsidies, designed to realign individual incentives with collective benefits.

A direct way to restore the attractiveness of the C-strategy in the *Landscape pooling* scenario would be to enable access to clean seeds at a lower price, subsidizing the cooperative contribution to disease dilution in the seed pool. We analysed this refined scenario and evidenced that, while a subsidy lowers the infection peak, overall dis-

ease suppression remains less effective than in the *Selective pooling* case because free-riding persists (Appendix H; Fig. 9). This result suggests that while subsidies do stimulate clean seed uptake, the public good nature of the landscape-scale seed pool dampens the marginal benefit of individual adoption because of free-riding. While landscape-scale seed pooling can, in principle, achieve superior bioeconomic performance than selective seed pooling (Fig. 6b., d.), its practical implementation in human-mediated systems yields outcomes that are less efficient than those produced by uncooperative selective seed-sharing network structures in terms of disease prevalence (Fig. 2c., f., and 3c., f.). Subsidies are insufficient to close the performance gap (Fig. 9), highlighting the need for more carefully designed interventions or management and governance structures.

A critical insight from our analysis is that, under the free-riding regime, more transmissible diseases trigger higher clean seed uptake, which subsequently tends to reduce disease prevalence (Fig. 3, 4, 7). Therefore, while introducing additional disease control measures would suppress the within-field infection rate, it would also erode the relative economic advantage for growers to invest in clean seeds, resulting in a decline in clean seed uptake, and ultimately triggering a counterintuitive increase in disease prevalence at landscape scale (Fig. 5, 8). Similar counterintuitive outcomes arising from complex behavioural-epidemiological feedback loops have been reported in the behavioural epidemiology literature. Notably, increased control efficacy can foster free-riding or reduce adherence to preventive measures, thereby undermining population-level disease suppression [10,14,45]. This phenomenon highlights that evaluating disease management strategies solely on epidemiological efficacy can be misleading if behavioural feedbacks are ignored.

Our results refine the classical understanding of the clean seed problem. Consistent with recent behavioural epidemiology studies, clean seed adoption might remain incomplete because of cost constraints and decentralized decision-making, leading to persistent disease even when effective control options are available [14]. Unlike existing models that often assume homogeneous uptake or overlook the feedbacks of seed system organization [17], our framework contrasts selective and landscape-scale seed pooling to reveal how institutional structures, as seed-sharing networks, can modulate disease suppression. We find that decentralized decision-making can achieve full clean seed adoption and eradicate the disease under favorable economic and institutional conditions, as low clean seed costs and restricted seed circulation. Yet, shared seed reservoirs create a public-good effect that dilutes infection pressure but might simultaneously stabilize mixed-control endemic states by incentivizing free-riding. Therefore, the clean seed problem is not only a bioeconomic issue but also an institutional one, with the mode of farmer seed circulation determining whether individual incentives translate into effective landscape-scale disease suppression.

Our framework relies on several simplifying assumptions designed to isolate the fundamental feedbacks between seed choice and seasonal transmission. By considering a closed metapopulation without explicit inter-field dispersal or external pathogen immigration, we prioritize the internal dynamics of the seed-system/behavioural loop. In this context, treating certified seeds as an idealized, pathogen-free baseline provides a clear benchmark for control efficacy, while the unmonitored exchange of farm-saved seeds captures key features of informal agricultural networks. While these simplifications ensure analytical tractability, they establish a baseline from which more realistic ecological and institutional complexities can be explored. For instance, the introduction of imperfect clean seed quality, spatial connectivity between fields, or logistical constraints on seed exchange would likely shift the adoption thresholds and the resilience of all-or-nothing ot free-riding regimes. Furthermore, the semi-discrete architecture of our framework is inherently modular, making it readily adaptable to other seasonal inter-

ventions such as crop rotation [27,46], the deployment of resistant varieties [36,37,47,48], or chemical seed treatments [49]. Considering these varied control modalities would allow for an exploration of synergistic or antagonistic effects between grower behaviour and seasonal plant disease epidemics.

A substantial body of literature focuses on identifying optimal disease control strategies from a top-down, central planner, perspective [36,37,50,51]. Our results highlight the difficulty of realizing such optima in decentralized grower populations. We evidence a persistent gap between individual behavioural choices and centralized objectives, whether aimed at minimizing landscape prevalence or maximizing total bioeconomic payoff (Fig. 6). Specifically, in the landscape pooling scenario, the bioeconomic optimum requires a higher level of clean-seed adoption than what emerges naturally from decentralized behaviour. However, reaching this optimum introduces a high degree of socio-economic unfairness: clean-seed users bear the cost of control, while farm-saved seed users gain a disproportionate relative advantage from the resulting lower infection pressure. Consequently, the behavioural equilibrium aligns with the bioeconomic and epidemiological optima only in the unrealistic scenario where clean seeds are provided at no cost. Achieving optimal control might therefore be less a technical problem than a governance challenge of steering decentralized incentives toward the collective good.

The modeling framework also highlights the role of behavioural assumptions. In particular, the imitation dynamics employed here capture bounded rationality and gradual adaptation through a flexibility parameter. Although the latter had no impact on the qualitative structure of the results, alternative specifications on the representation of grower behavioural adaptation, such as nonlinear imitation rules, risk-sensitive decision-making, or utility-based choice models, could lead to different outcomes [52,53]. In practice, growers rarely possess complete or precise information regarding infection risk, yield loss, and the effectiveness of control measures [54]. To capture this realism, our semi-discrete framework can be readily extended to incorporate payoff uncertainty by allowing growers to evaluate strategies based on noisy payoff estimates at the end of each season, and to update their choices via imitation driven by expected utility rather than realized payoff. This approach naturally accommodates heterogeneity in risk preferences, ranging from risk-averse individuals who prioritize stable outcomes to risk-prone individuals willing to tolerate uncertainty for potentially larger gains [55]. Incorporating such payoff uncertainty would provide a more realistic foundation for investigating how imperfect information in seasonal disease conditions and heterogeneous risk attitudes of growers shape decision-making and, in turn, influence disease dynamics.

Finally, although this study focuses on plant disease systems, the underlying mechanisms are more general. Many epidemiological settings involve seasonal decision-making, delayed feedbacks, and interactions between individual behaviour and collective risk. For instance, seasonal influenza vaccination decisions are typically made prior to the onset of the epidemic, often in early autumn in temperate regions, with uptake influenced by the perceived risk, expected vaccine effectiveness, and the epidemiological memory of recent outbreaks. This creates a feedback loop where past disease severity shapes current behaviour, which in turn affects future transmission dynamics. Similar patterns arise in vector-borne diseases like dengue fever, where protective actions intensify during high-risk seasons based on recent exposure levels. Extending the semi-discrete framework developed here to such contexts may provide new insights into how timing constraints shape behavioural-epidemiological dynamics more broadly.

5 ACKNOWLEDGEMENTS

We acknowledge funding from the ANR project BEEP (Behavioural Epidemiology and Evolution of Plant Pathogens), grant number ANR-23-CE35-0012, and from the INRAE - University of Florida Joint Linkage Call 2023 project INAPP (Impact Network Analysis for containing invasive soilborne Pathogens and Pests). FMHi acknowledges partial support by Deutsche Forschungsgemeinschaft (DFG, German Research Foundation) [project number 518865889]. We thank Jonas Wahl for introducing us to trans-heteroclinic bifurcations and related references.

REFERENCES

[1] Serge Savary, Laetitia Willocquet, Sarah Jane Pethybridge, Paul Esker, Neil McRoberts, and Andy Nelson. The global burden of pathogens and pests on major food crops. *Nature ecology & evolution*, 3(3):430–439, 2019.

[2] H Charles J Godfray, John R Beddington, Ian R Crute, Lawrence Haddad, David Lawrence, James F Muir, Jules Pretty, Sherman Robinson, Sandy M Thomas, and Camilla Toulmin. Food security: the challenge of feeding 9 billion people. *science*, 327(5967):812–818, 2010.

[3] James F Sallis, Neville Owen, and Michael J Fotheringham. Behavioral epidemiology: a systematic framework to classify phases of research on health promotion and disease prevention. *Annals of behavioral medicine*, 22(4):294–298, 2000.

[4] Piero Manfredi and Alberto D'Onofrio. *Modeling the interplay between human behavior and the spread of infectious diseases*. Springer Science & Business Media, 2013.

[5] Chris T Bauch. Imitation dynamics predict vaccinating behaviour. *Proceedings of the Royal Society B: Biological Sciences*, 272(1573):1669–1675, 2005.

[6] Chris T Bauch and David JD Earn. Vaccination and the theory of games. *Proceedings of the National Academy of Sciences U.S.A.*, 101(36):13391–13394, 2004.

[7] Sebastian Funk, Marcel Salathé, and Vincent AA Jansen. Modelling the influence of human behaviour on the spread of infectious diseases: a review. *Journal of the Royal Society Interface*, 7(50):1247–1256, 2010.

[8] Tamer Oraby, Vivek Thampi, and Chris T Bauch. The influence of social norms on the dynamics of vaccinating behaviour for paediatric infectious diseases. *Proceedings of the Royal Society B: Biological Sciences*, 281(1780), 2014.

[9] Hugo Martin, François Castella, and Frédéric Hamelin. Wearing face masks to protect oneself and/or others: Counter-intuitive results from a simple epidemic model accounting for selfish and altruistic human behaviour. 2025.

[10] Chadi M Saad-Roy and Arne Traulsen. Dynamics in a behavioral–epidemiological model for individual adherence to a nonpharmaceutical intervention. *Proceedings of the National Academy of Sciences U.S.A.*, 120(44):e2311584120, 2023.

[11] Alice E Milne, James R Bell, William D Hutchison, Frank van den Bosch, Paul D Mitchell, David Crowder, Stephen Parnell, and Andrew P Whitmore. The effect of farmers' decisions on pest control with bt crops: a billion dollar game of strategy. *PLoS computational biology*, 11(12):e1004483, 2015.

[12] Nadine Aschauer and Stephen Parnell. Analysis of mathematical modelling approaches to capture human behaviour dynamics in agricultural pest and disease systems. *Agricultural Systems*, 226:104303, 2025.

[13] Rachel E. Murray-Watson, Frédéric M. Hamelin, and Nik J. Cunniffe. How growers make decisions impacts plant disease control. *PLOS Computational Biology*, 18(8):1–27, 08 2022.

[14] Rachel E Murray-Watson and Nik J Cunniffe. Expanding growers' choice of plant disease management options can promote suboptimal social outcomes. *Plant Pathology*, 72(5):933–950, 2023.

[15] Alice E Milne, Tim Gottwald, Stephen R Parnell, Vasthi Alonso Chavez, and Frank Van den Bosch. What makes or breaks a campaign to stop an invading plant pathogen? *PLOS Computational Biology*, 16(2):e1007570, 2020.

[16] Anna Maria Szyniszewska, Patrick Chiza Chikoti, Mathias Tembo, Rabson Mulenga, Christopher Aidan Gilligan, Frank van den Bosch, and Christopher Finn McQuaid. Cassava planting material movement and grower behaviour in zambia: implications for disease management. *BioRxiv*, page 528851, 2019.

[17] Christopher Finn McQuaid, Christopher Aidan Gilligan, and Frank van den Bosch. Considering behaviour to ensure the success of a disease control strategy. *Royal Society Open Science*, 4(12), 2017.

[18] Yuji Saikai, Terrance M Hurley, and Paul D Mitchell. An agent-based model of insect resistance management and mitigation for bt maize: a social science perspective. *Pest Management Science*, 77(1):273–284, 2021.

[19] Frédéric M Hamelin, Magda Castel, Sylvain Poggi, Didier Andrivon, and Ludovic Mailleret. Seasonality and the evolutionary divergence of plant parasites. *Ecology*, 92(12):2159–2166, 2011.

[20] L Bos. Crop losses caused by viruses. *Crop Protection*, 1(3):263–282, 1982.

[21] Shawn McGuire and Louise Sperling. Seed systems smallholder farmers use. *Food security*, 8(1):179–195, 2016.

[22] Israel Pagán. Transmission through seeds: The unknown life of plant viruses. *PLoS Pathogens*, 18(8):e1010707, 2022.

[23] Christopher A Gilligan. Sustainable agriculture and plant diseases: an epidemiological perspective. *Philosophical Transactions of the Royal Society B: Biological Sciences*, 363(1492):741–759, 2008.

[24] Rachel E Murray-Watson and Nik J Cunniffe. How the epidemiology of disease-resistant and disease-tolerant varieties affects grower behaviour. *Journal of the Royal Society Interface*, 19(195), 2022.

[25] Frank M Hilker, Lea-Deborah Kolb, and Frédéric M Hamelin. Selfish grower behavior can group-optimally eradicate plant diseases caused by coinfection. *International Game Theory Review*, 26(02):2440006, 2024.

[26] Kenneth E Frost, Russell L Groves, and Amy O Charkowski. Integrated control of potato pathogens through seed potato certification and provision of clean seed potatoes. *Plant disease*, 97(10):1268–1280, 2013.

[27] Frank M Hilker, Linda JS Allen, Vrushali A Bokil, Cheryl J Briggs, Zhilan Feng, Karen A Garrett, Louis J Gross, Frédéric M Hamelin, Michael J Jeger, Carrie A Manore, et al. Modeling virus coinfection to inform management of maize lethal necrosis in kenya. *Phytopathology*, 107(10):1095–1108, 2017.

[28] James KM Brown. Yield penalties of disease resistance in crops. *Current opinion in plant biology*, 5(4):339–344, 2002.

[29] Oliver T Coomes, Shawn J McGuire, Eric Garine, Sophie Caillon, Doyle McKey, Elise Demeulenaere, Devra Jarvis, Guntra Aistara, Adeline Barnaud, Pascal Clouvel, et al. Farmer seed networks make a limited contribution to agriculture? four common misconceptions. *Food Policy*, 56:41–50, 2015.

[30] Sara Thomas-Sharma, Jorge Andrade-Piedra, Mónica Carvajal Yepes, JF Hernandez Nopsa, MJ Jeger, RAC Jones, Peter Kromann, James P Legg, Jonathan Yuen, GA Forbes, et al. A risk assessment framework for seed degeneration: Informing an integrated seed health strategy for vegetatively propagated crops. *Phytopathology*, 107(10):1123–1135, 2017.

[31] Nicolas WG Chen, Mylène Ruh, Armelle Darrasse, Justine Foucher, Martial Briand, Joana Costa, David J Studholme, and Marie-Agnès Jacques. Common bacterial blight of bean: a model of seed transmission and pathological convergence. *Molecular Plant Pathology*, 22(12):1464–1480, 2021.

[32] Kelsey F. Andersen Onofre, Erik Delaquis, Jonathan C. Newby, Stef de Haan, Cu Thi Le Thuy, Nami Minato, James P. Legg, Wilmer J. Cuellar, Ricardo I. Alcalá Briseño, and Karen A. Garrett. Decision support for managing an invasive pathogen through efficient clean seed systems: Cassava mosaic disease in southeast asia. *Agricultural Systems*, 229:104435, 2025.

[33] Josef Hofbauer and Karl Sigmund. Evolutionary game dynamics. *Bulletin of the American mathematical society*, 40(4):479–519, 2003.

[34] Ludovic Mailleret and Valérie Lemesle. A note on semi-discrete modelling in the life sciences. *Philosophical Transactions of the Royal Society A: Mathematical, Physical and Engineering Sciences*, 367(1908):4779–4799, 2009.

[35] Ludovic Mailleret, Magda Castel, Josselin Montarry, and Frédéric M Hamelin. From elaborate to compact seasonal plant epidemic models and back: is competitive exclusion in the details? *Theoretical ecology*, 5:311–324, 2012.

[36] Frederic Fabre, Elsa Rousseau, Ludovic Mailleret, and Benoit Moury. Durable strategies to deploy plant resistance in agricultural landscapes. *New Phytologist*, 193(4):1064–1075, 2012.

[37] Frédéric Fabre, Elsa Rousseau, Ludovic Mailleret, and Benoît Moury. Epidemiological and evolutionary management of plant resistance: optimizing the deployment of cultivar mixtures in time and space in agricultural landscapes. *Evolutionary Applications*, 8(10):919–932, 2015.

[38] Collective. Farmer seed systems: A critical contribution to food sovereignty and farmers' rights. Technical report, SeedChange, 2020.

[39] Yin-Wong Cheung and Daniel Friedman. A comparison of learning and replicator dynamics using experimental data. *Journal of economic behavior & organization*, 35(3):263–280, 1998.

[40] Akiko Satake and Yoh Iwasa. Coupled ecological and social dynamics in a forested landscape: the deviation of individual decisions from the social optimum. *Ecological Research*, 21:370–379, 2006.

[41] Carl Brusse and Justin Bruner. Responsiveness and robustness in the david lewis signalling game. *Philosophy of Science*, 84(5):1068–1079, 2017.

[42] Joana G Vicente and Eric B Holub. Xanthomonas campestris pv. campestris (cause of black rot of crucifers) in the genomic era is still a worldwide threat to brassica crops. *Molecular plant pathology*, 14(1):2–18, 2013.

[43] RX Latin and DL Hopkins. Bacterial fruit blotch of watermelon: The hypothetical exam question becomes reality. *Plant Disease*, 79:761–765, 1995.

[44] Elias Koutsoupias and Christos Papadimitriou. Worst-case equilibria. *Computer science review*, 3(2):65–69, 2009.

[45] Chris T Bauch, Samit Bhattacharyya, and Robert F Ball. Rapid emergence of free-riding behavior in new pediatric immunization programs. *PLoS One*, 5(9):e12594, 2010.

[46] Maria Bargués-Ribera and Chaitanya S Gokhale. Eco-evolutionary agriculture: Host-pathogen dynamics in crop rotations. *PLoS computational biology*, 16(1):e1007546, 2020.

[47] Bruce A McDonald and Celeste Linde. The population genetics of plant pathogens and breeding strategies for durable resistance. *Euphytica*, 124(2):163–180, 2002.

[48] Samuel Nilusmas, Mathilde Mercat, Thomas Perrot, Caroline Djian-Caporalino, Philippe Castagnone-Sereno, Suzanne Touzeau, Vincent Calcagno, and Ludovic Mailleret. Multi-seasonal modelling of plant-nematode interactions reveals efficient plant resistance deployment strategies. *Evolutionary applications*, 13(9):2206–2221, 2020.

[49] Denis C McGee. Epidemiological approach to disease management through seed technology. *Annual review of phytopathology*, 33(1):445–466, 1995.

[50] Graeme A Forster and Christopher A Gilligan. Optimizing the control of disease infestations at the landscape scale. *Proceedings of the National Academy of Sciences*, 104(12):4984–4989, 2007.

[51] Robert E Rowthorn, Ramanan Laxminarayan, and Christopher A Gilligan. Optimal control of epidemics in metapopulations. *Journal of the Royal Society Interface*, 6(41):1135, 2009.

[52] György Szabó and Csaba Tőke. Evolutionary prisoner's dilemma game on a square lattice. *Physical Review E*, 58(1):69, 1998.

[53] Arne Traulsen and Christoph Hauert. Stochastic evolutionary game dynamics. *Reviews of nonlinear dynamics and complexity*, 2:25–61, 2009.

[54] Haim Levy. Absolute and relative risk aversion: An experimental study. *Journal of Risk and uncertainty*, 8(3):289–307, 1994.

[55] Guocheng Wang, Qi Su, Long Wang, and Joshua B Plotkin. The evolution of social behaviors and risk preferences in settings with uncertainty. *Proceedings of the National Academy of Sciences*, 121(30):e2406993121, 2024.

[56] Nicoletta Bof, Ruggero Carli, and Luca Schenato. Lyapunov theory for discrete time systems. *arXiv preprint arXiv:1809.05289*, 2018.

[57] Josep Sardanyés, Regina Martínez, and Carles Simó. Trans-heteroclinic bifurcation: a novel type of catastrophic shift. *Royal Society Open Science*, 5(1), 2018.

[58] Katsuhiko Ogata. *Discrete-time control systems*. Prentice-Hall, Inc., 1995.

A DISEASE PREVALENCE

Prevalence at field scale

Let P_c and P_f denote the prevalence in a C-field and F-field, respectively. By definition $P_z = \frac{I_z}{N}$ for $z = c, f$ so that, from Equation 2, in-season dynamics can be written in terms of disease prevalence:

$$\begin{aligned}\dot{P}_z &= \tfrac{1}{N}\left[\beta(N - I_z)I_z + \gamma(N - I_z)((1 - p_k)nI_f + p_k nI_c)\right], \\ &= \beta N(1 - P_z)P_z + \gamma N(1 - P_z)((1 - p_k)nP_f + p_k nP_c),\end{aligned}$$

which are the very same equations as Equation 2, up to a standard mutliplication of infection rates by N.

The proportion of C-fields p_{k+1} can also be expressed in terms of prevalences. Indeed, from Equations (3), (4) and (5):

$$\begin{aligned}p_{k+1} &= s\frac{g(N - I_{c,k}) + (1 - \delta)gI_{c,k} - cN}{(1 - p_k)(g(N - I_{f,k}) + (1 - \delta)gI_{f,k}) + p_k(g(N - I_{c,k}) + (1 - \delta)gI_{c,k} - cN)}p_k + (1 - s)p_k, \\ &= s\frac{g(1 - P_{c,k}) + (1 - \delta)gP_{c,k} - c}{(1 - p_k)(g(1 - P_{f,k}) + (1 - \delta)gP_{f,k}) + p_k(g(1 - P_{c,k}) + (1 - \delta)gP_{c,k} - c)}p_k + (1 - s)p_k.\end{aligned}$$

Finally, between season transition Equations (6), (7) and (8) are the same in terms of prevalence than in terms of infected plants, because of the multiplicative scaling by N.

Prevalence at landscape scale

The number of infected plants at landscape scale is equal to the number of fields of a given type, times the number of infected plants in that field type:

$$I_\ell = p_k nI_c + (1 - p_k)nI_f.$$

Therefore, the prevalence at landscape scale, defined as $P_\ell = \frac{I_\ell}{nN}$, is equal to:

$$P_\ell = p_k P_c + (1 - p_k)P_f.$$

B REDUCED MODELS

The negligible between field transmission hypothesis $\gamma = 0$ brings about several simplifications that allow for a comprehensive mathematical analysis of model dynamics. The first direct consequence is that $I_c(t) = 0$ at any time, for $I_c(kT) = 0$ being an equilibrium of the $\dot{I}_c$ equation in (2). Therefore, the performance of the clean seed strategy (Eq. 3) is directly determined by the balance between the cost of clean seeds and the profit from mature plants:

$$\Pi_{c,k} = (g - c)N, \tag{B.1}$$

Furthermore, disease dynamics in F-fields simplify into the autonomous equation:

$$\dot{I}_f = \beta(N - I_f)I_f. \tag{B.2}$$

From Eq. (5), the proportion of C-fields in cropping cycle $(k+1)$ are thus determined by epidemic dynamics in F-fields only:

$$\begin{aligned} p_{k+1} &= \left(\frac{s(g-c)N}{(1-p_k)g(N-\delta I_{f,k}) + p_k(g-c)N} + (1-s)\right) p_k, \\ &= \left(\frac{s(g-c)N}{(g-p_k c)N - (1-p_k)\delta g I_{f,k}} + (1-s)\right) p_k, \end{aligned} \tag{B.3}$$

Further simplifications depend on the considered scenario.

Selective seed pooling

In the *Selective seed pooling* scenario, $I_f((k+1)T)$ is equal to $\nu I_{f,k}$ (Eq. 7) that is independent of p_{k+1}. Epidemic dynamics in F-fields then obey the simple autonomous semi-discrete equations:

$$\begin{aligned} \dot{I}_f &= \beta(N - I_f)I_f, \text{ for } t \in [kT, kT+\tau] \\ I_f((k+1)T) &= \nu I_f(kT+\tau). \end{aligned} \tag{B.4}$$

The dynamics of clean seed uptake at the metapopulation scale are thus fully determined by Equation (B.3), and have no influence on within F-field disease dynamics (Equation B.4).

Landscape seed pooling

In the *Landscape seed pooling* scenario, $I_f((k+1)T)$ depends on both p_k and $I_{f,k}$, so that the proportion of growers opting for clean seed in the previous cropping cycle actually influences disease dynamics in F-fields in the next cycle. Thus, over cropping cycles, there are direct feedbacks between the clean seed strategy and the epidemics at field scale, which transfer to the metapopulation scale. In that scenario, epidemic dynamics in F-fields follow the semi-discrete equations:

$$\begin{aligned} \dot{I}_f &= \beta(N - I_f)I_f, \text{ for } t \in [kT, kT+\tau] \\ I_f((k+1)T) &= \nu(1-p_k)I_f(kT+\tau), \end{aligned} \tag{B.5}$$

with p_k determined from the $(k-1)$th cropping cycle according to Equation (B.3).

C ANALYSIS OF THE SELECTIVE SEED POOLING SCENARIO

In what follows, we study the asymptotic properties of the model (B.3) and (B.4) in terms of the year-to-year mapping of state variables at the end of season, *i.e.* at $t = kT + \tau$. At that scale, the stationary periodic solutions (as the periodic epidemics illustrated in Fig. 1) correspond to year-to-year fixed points; the properties of the semi-discrete model are then analyzed through discrete time dynamical systems tools[56].

In the *Selective seed pooling* scenario, under the $\gamma = 0$ hypothesis, the dynamics follow Equations (B.4); the proportion of C-fields at landscape scale, and therefore disease dynamics at landscape scale, simply derive from those dynamics and do not interact with them.

Disease dynamics in F-fields

Integrating the $\dot{I}_f$ equation in Eq. (B.4) between $t = (k+1)T$ and $(k+1)T + \tau$ yields:

$$I_{f,k+1} = I_f((k+1)T + \tau) = \frac{N\, I_f((k+1)T) e^{\beta N \tau}}{N + I_f((k+1)T)(e^{\beta N \tau} - 1)}, \tag{C.1}$$

so that, using the second equation in (B.4):

$$I_{f,k+1} = \frac{N \nu I_{f,k} e^{\beta N \tau}}{N + \nu I_{f,k}(e^{\beta N \tau} - 1)}. \tag{C.2}$$

Fixed points (equilibria) of this sequence correspond either to disease clearance (disease free equilibrium (DFE): $I_f = 0$), or to an endemic equilibrium (EE) such that:

$$I_f^* = \frac{\nu h - 1}{\nu(h-1)} N, \tag{C.3}$$

using the shorthand notation $h = e^{\beta N \tau}$ for the seasonal reproductive factor of the disease corresponding to horizontal transmission.

The endemic equilibrium I_f^* is not necessarily biologically feasible. It is smaller or equal to N if and only if $\nu \leq 1$ (which is true since ν is a proportion). It is positive if the season-to-season reproduction number of the disease, that accounts for the transmission through seeds, is such that:

$$\mathcal{R}_0 = \nu h > 1.$$

For the interest of the study, we mostly focus on cases where the disease is not simply wiped out because of low transmission capacities, i.e. we assume that the latter equation is true. Standard tools on dimension 1 mappings then directly show that I_f^* is (globally) asymptotically stable and $I_f = 0$ is unstable in that case. Otherwise, $I_f = 0$ is (globally) asymptotically stable.

Behavioural dynamics

Fixed points for the proportion of C-fields when F-fields are at endemic equilibrium are computed from Equation (B.3) with $I_{f,k} = I_f^*$. They are solutions of:

$$p = \left(\frac{s(g-c)N}{(g - pc)N - (1-p)\delta g I_f^*} + (1-s) \right) p.$$

Thus, either $p = 0$ (no use of clean seeds, *i.e.* no control), or:

$$(g - pc)N - (1-p)\delta g I_f^* = (g-c)N,$$

that is, using Equation (C.3):

$$(1-p)c = (1-p)\delta g \frac{\nu h - 1}{\nu(h-1)},$$

so that either $\frac{c}{\delta g} = \frac{\nu h-1}{\nu(h-1)}$, or $p = 1$. In the particular case that $\frac{c}{\delta g} = \frac{\nu h-1}{\nu(h-1)}$, any $p \in [0, 1]$ defines an equilibrium.

To summarize, when $\frac{c}{\delta g} \neq \frac{\nu h-1}{\nu(h-1)}$, the model admits four year-to-year fixed points at $t = kT + \tau$ such that $(I_f, p) = (0, 0)$ (DFE - no control), $(0, 1)$ (DFE - full control), $(I_f^*, 0)$ (EE - no control) and $(I_f^*, 1)$ (EE - full control). The former two equilibria always exist, while the latter two exist only when $\mathcal{R}_0 > 1$. When $\mathcal{R}_0 > 1$ and $\frac{c}{\delta g} = \frac{\nu h-1}{\nu(h-1)}$, there exists in addition a continuum of equilibria (I_f^*, p) for any $p \in [0, 1]$, that connects the EE - no control equilibrium to the EE - full control equilibrium.

Stability analysis

With $\mathcal{R}_0 > 1$, the DFE in (C.2) is unstable; the equilibria associated with the DFE, $(0, 0)$ and $(0, 1)$, are unstable too.

Moreover, since the EE is asymptotically stable independently of clean seed uptake p_k, the stability of EE associated equilibria can be studied in dimension 1, focusing on p_k dynamics. An equilibrium is therefore asymptotically stable if $\left|\frac{\partial p_{k+1}}{\partial p_k}\right|$ evaluated at that equilibrium is smaller than 1.

From Eq. (B.3), we have:

$$\frac{\partial p_{k+1}}{\partial p_k} = (1-s) + s(g-c)N\frac{(g-p_k c)N - (1-p_k)\delta g I_{f,k} - p_k[-cN + \delta g I_{f,k}]}{[(g-p_k c)N - (1-p_k)\delta g I_{f,k}]^2}. \tag{C.4}$$

Therefore, at the EE - no control equilibrium:

$$\frac{\partial p_{k+1}}{\partial p_k}(I_f = I_f^*, p = 0) = (1-s) + s\frac{(g-c)N}{gN - \delta g I_f^*} \tag{C.5}$$

From the application viewpoint, we assume that the gain earned from a healthy plant is larger than the cost of a clean seed plant, *i.e.* $g > c$. Furthermore, δ and s are proportions and $I_f^* < N$ by definition, so that (C.5) is positive. Using Eq. (C.3), the derivative (C.5) is smaller than 1 if:

$$\frac{(g-c)N}{g(N-\delta I_f^*)} < 1 \Leftrightarrow \frac{c}{\delta g} > \frac{\nu h - 1}{\nu(h-1)}, \tag{C.6}$$

and larger than 1 if the inequality is reversed.

Therefore, the EE - no control equilibrium is asymptotically stable when inequality (C.6) holds true, and unstable when it is reversed.

At the EE - full control equilibrium, Eq. (C.4) yields:

$$\frac{\partial p_{k+1}}{\partial p_k}(I_f = I_f^*, p = 1) = (1-s) + s\frac{g(N-\delta I_f^*)}{(g-c)N}, \tag{C.7}$$

which is positive, using the same arguments as for Eq. (C.5), and smaller than 1 provided:

$$\frac{g(N-\delta I_f^*)}{(g-c)N} < 1 \Leftrightarrow \frac{c}{\delta g} < \frac{\nu h - 1}{\nu(h-1)}.$$

This is exactly inequality (C.6) reversed, so that the EE - full control equilibrium is unstable when C.6 holds true, and asymptotically stable when it is reversed.

At the bifurcation, when $\frac{c}{\delta g} = \frac{\nu h - 1}{\nu(h-1)}$, the continuum of equilibria (I_f^*, p) is neutrally stable, connecting the stable EE – no control equilibrium when (C.6) holds true to the stable EE – full control when (C.6) is reversed. This peculiar bifurcation is the discrete-time analogous to a "trans-heteroclinic bifurcation" that has been recently put forward in continuous time dynamical systems[57]. It generates abrupt changes in the asymptotic dynamics of the model, similar to what saddle-node bifurcations and tipping points usually entail (Fig. 2a.-c. and 3a.-c.).

Summary

To sum up, in the *Selective seed pooling* scenario when $\mathcal{R}_0 > 1$, the model admits four year-to-year equilibria at $t = kT + \tau$: the DFE - no control and DFE - full control equilibria, which are both unstable, and the EE - no control and EE - full control equilibria. The stability of the latter two equilibria are determined by an additional condition involving, among others, the cost of clean seeds c, and the disease transmission capacities $h = e^{\beta N \tau}$ and ν.

When inequality (C.6) holds true, the EE - no control equilibrium is asymptotically stable and the other is unstable. When (C.6) is reversed, the EE - full control equilibrium is asymptotically stable and the other is unstable.

Interestingly, condition (C.6) can be further interpreted in terms of comparison between the F- and C- strategies associated costs ($p = 0$ and 1, respectively). Indeed, (C.6) is equivalent to:

$$cN > \delta g I_f^*.$$

Therefore, the selection between the F- and C- strategies relies on a quantitative comparison between the cost of clean seeds in a C-field (cN) and the cost entailed by the disease in an F-field at the EE - no control equilibrium ($\delta g I_f^*$).

Finally, when $\mathcal{R}_0 < 1$, there are only two equilibria, that correspond to disease clearance. In that case, the DFE - no control equilibrium is asymptotically stable, and the DFE - full control equilibrium is unstable (not shown).

At the metapopulation scale, existence and stability conditions of equilibria follow from the above analysis. The DFE - no control situation translates into a landscape of disease free F-fields, and the DFE - full control into a landscape of C-fields (that are also disease-free). The EE - full control situation also corresponds to a landscape of disease-free C-fields; indeed, with $p_k = 1$ the EE in F-fields remain virtual and do not impact landscape scale prevalence. The last EE - no control situation results in a landscape of F-fields at EE.

The different regimes of asymptotic dynamics are illustrated with respect to clean seed cost c on Figure 2 (left column) and with respect to horizontal reproduction factor $h = e^{\beta N \tau}$ on Figure 3 (left column).

D ANALYSIS OF THE LANDSCAPE SEED POOLING SCENARIO

In the *Landscape seed pooling* scenario, disease dynamics in F-fields (Eqs. B.5) are directly in interaction with the dynamics of clean seed uptake across the landscape (Eq. B.3). A two-step analysis, as in appendix C, is therefore not possible and the full 2-dimensional semi-discrete model has to be taken into account to solve for fixed points and to assess stability. Nonetheless, the core of the analysis still relies on studying the year-to-year mapping of state variables.

Coupled disease - behaviour dynamics

As in the *Selective seed pooling* scenario, Equation (C.1) holds so that using the second equation in B.5 together with Eq. (B.3), the full semi-discrete model is summarized by the following discrete-time system at times $t = (k+1)T + \tau$:

$$\begin{aligned} I_{f,k+1} &= \frac{N\nu h(1-p_k)I_{f,k}}{N+\nu(h-1)(1-p_k)I_{f,k}}, \\ p_{k+1} &= \left(\frac{s(g-c)N}{(g-p_kc)N-(1-p_k)\delta g I_{f,k}} + (1-s)\right)p_k, \end{aligned} \tag{D.1}$$

retaining the notation $h = e^{\beta N\tau}$.

Fixed points of this system thus verify:

$$\begin{aligned} &I_f = 0, \text{ or } N\nu h(1-p) = N + \nu(h-1)(1-p)I_f, \\ &\text{and} \\ &p = 0, \text{ or } p = 1, \text{ or } I_f = I^*_{f,m} = \tfrac{cN}{\delta g}. \end{aligned} \tag{D.2}$$

Two of the six possibilities lead to contradictions, so that there remain four possible fixed points:

- DFE - no control $(I_f, p) = (0, 0)$
- DFE - full control $(I_f, p) = (0, 1)$
- EE - no control $(I_f, p) = (I^*_f, 0)$, with I^*_f defined in Eq. (C.3)
- a different EE, with mixed control $(I_f, p) = (I^*_{f,m}, p^*_m)$

The two former equilibria always exist, and the third exists provided the year-to-year reproduction number of the disease $\mathcal{R}_0$ is greater than 1 (see Appendix C).

For the latter EE - mixed control equilibrium to be biologically feasible, it is firstly required that p^*_m lies between 0 and 1. One gets from the second condition in the first equation of (D.2):

$$p^*_m = 1 - \frac{\delta g}{\nu(h(\delta g - c) + c)}, \tag{D.3}$$

The positivity condition on p^*_m is equivalent to:

$$\delta g < \nu(h(\delta g - c) + c) \;\Leftrightarrow\; \delta g(\nu h - 1) > \nu c(h-1).$$

When $\mathcal{R}_0 < 1$, this condition can never be met, while when $\mathcal{R}_0 > 1$ the condition holds iff:

$$\frac{c}{\delta g} < \frac{\nu h - 1}{\nu(h-1)}, \tag{D.4}$$

which is exactly Eq. (C.6) reversed, and can also be written as:

$$I^*_{f,m} < I^*_f.$$

When (D.4) holds, then $c < \delta g$ because the RHS is smaller than 1 since $\nu < 1$. Thus, both $I^*_{f,m} < N$ and $p^*_m < 1$.

Therefore, the EE - mixed control equilibrium $(I^*_{f,m}, p^*_m)$ exists if and only if $\mathcal{R}_0 > 1$ and condition (D.4) holds true.

Stability analysis

From the year-to-year mapping (D.1), one can compute the general form of the Jacobian matrix at $(I_{f,k}, p_k)$:

$$J = \begin{pmatrix} \frac{N^2\nu h}{\Theta^2}(1-p_k) & -\frac{N^2\nu h}{\Theta^2} I_{f,k} \\ \frac{s(g-c)N}{\Xi^2}\delta g p_k(1-p_k) & \frac{s(g-c)N}{\Xi^2}(gN - \delta g I_{f,k}) + (1-s) \end{pmatrix}, \tag{D.5}$$

with:

$$\Theta = N + \nu(h-1)(1-p_k)I_{f,k},$$
and
$$\Xi = (g - p_k c)N - (1-p_k)\delta g I_{f,k}.$$

At the DFE - no control equilibrium, the Jacobian reads:

$$J(0,0) = \begin{pmatrix} \nu h & 0 \\ 0 & 1 - \frac{sc}{g} \end{pmatrix}.$$

The first eigenvalue is $\mathcal{R}_0$, while the second lies strictly between 0 and 1, from the assumptions that $g > c$ and $s \in (0, 1]$. Therefore, the DFE - no control equilibrium is asymptotically stable when $\mathcal{R}_0 < 1$, and unstable when it is larger than 1.

At the DFE - full control equilibrium, the Jacobian matrix reads:

$$J(0,1) = \begin{pmatrix} 0 & 0 \\ 0 & \frac{sc}{g-c} + 1 \end{pmatrix}.$$

The first eigenvalue is 0 and the second is larger than 1 since $g > c$ and $s > 0$. Therefore, the DFE - full control equilibrium is always unstable.

At the EE - no control equilibrium, the Jacobian matrix reads:

$$J(I^*_f, 0) = \begin{pmatrix} \frac{1}{\nu h} & * \\ 0 & \frac{s(g-c)}{g - \delta g \frac{\nu h - 1}{\nu(h-1)}} + (1-s) \end{pmatrix}.$$

The upper diagonal term is not needed for the stability analysis, so it is not computed explicitly. The first eigenvalue is $1/\mathcal{R}_0$, so it lies between 0 and 1 when the equilibrium exists. The second eigenvalue is positive since:

$$\frac{(g-c)}{g - \delta g \frac{\nu h - 1}{\nu(h-1)}} > 0.$$

Indeed, $g > c$, and both $\delta < 1$ and $\frac{\nu h - 1}{\nu(h-1)} < 1$, the latter being true since $\nu < 1$.

The second eigenvalue is larger than one when $\frac{(g-c)}{g-\delta g\frac{\nu h-1}{\nu(h-1)}}$ is, which is equivalent to the EE - mixed control equilibrium existence condition (D.4); it is smaller than one otherwise.

Therefore, the EE - no control is asymptotically stable when it exists ($\mathcal{R}_0 > 1$) and the EE - mixed control equilibrium does not exist. It is unstable when the EE - mixed control equilibrium exists (Eq. D.4).

At the EE - mixed control equilibrium, one gets the following Jacobian matrix after some algebra:

$$J(I^*_{f,m}, p^*_m) = \begin{pmatrix} 1 - \frac{(h-1)c}{h\delta g} & -\frac{cN\nu(h(\delta g-c)+c)^2}{h(\delta g)^3} \\ \frac{s(\delta g)^2(\delta g(\nu h-1)-c\nu(h-1))}{(g-c)N\nu^2(h(\delta g-c)+c)^2} & 1 \end{pmatrix}.$$

Stability analysis of this matrix is not as straightforward as above and goes through the study of Jury conditions[58] which state that, in dimension 2, matrix J has all its eigenvalues within the unit circle if and only if:

- $1 - \mathrm{tr}(J) + \det(J) > 0$,
- $1 + \mathrm{tr}(J) + \det(J) > 0$, and,
- $1 - \det(J) > 0$.

Here we have $\mathrm{tr}(J(I^*_{f,m}, p^*_m)) = 2 - \frac{(h-1)c}{h\delta g}$, and:

$$\det(J(I^*_{f,m}, p^*_m)) = 1 - \frac{(h-1)c}{h\delta g} + s\Gamma, \text{ with: } \Gamma = \frac{c(\delta g(\nu h-1) - c\nu(h-1))}{\nu h\delta g(g-c)}.$$

The first Jury condition simplifies to $s\Gamma > 0$, which is actually equivalent to the EE - mixed control equilibrium existence condition Eq. (D.4) since $g > c$.

The second condition holds true as well since the property $\delta g > c$, which is entailed by D.4, immediately implies that: $\mathrm{tr}(J(I^*_{f,m}, p^*_m)) > 0$.

The third condition is equivalent to $\frac{(h-1)c}{h\delta g} > s\Gamma$, which simplifies to:

$$(h-1) > s\frac{(\delta g(\nu h-1) - c\nu(h-1))}{\nu(g-c)},$$

which is equivalent to:

$$\frac{g-(1-s)c}{s\delta g} > \frac{\nu h-1}{\nu(h-1)}. \tag{D.6}$$

On the one hand, the left-hand side of (D.6) is decreasing in s; indeed:

$$\frac{d}{ds}\left(\frac{g-(1-s)c}{s\delta g}\right) = \frac{c-g}{s^2\delta g} < 0,$$

because $g > c$. Furthermore, when $s = 1$ the LHS of (D.6) reduces to $\frac{1}{\delta}$, which is larger than 1. Therefore, the LHS of (D.6) is larger than 1 for any $s \in [0, 1]$.

On the other hand, the RHS of (D.6) is lower than 1 since $\nu < 1$. Thus, the third Jury condition holds true.

Finally, when it exists, *i.e.* when (D.4) holds, the EE - mixed control equilibrium is asymptotically stable.

Summary

To sum up, in the *Landscape seed pooling* scenario when $\mathcal{R}_0 > 1$, there are at least three steady states at $t = kT + \tau$: the DFE - no control $(I_f, p) = (0, 0)$, the DFE - full control $(I_f, p) = (0, 1)$ and an EE - no control $(I_f, p) = (I_f^*, 0)$ equilibrium. DFE associated equilibria are always unstable in that case.

When condition D.4 is reversed, there is no other equilibrium and the EE - no control equilibrium is asymptotically stable. If condition D.4 holds true, there is an additional EE - mixed control equilibrium $(I_f, p) = (I_{f,m}^*, p_m^*)$, with $I_{f,m}^* < I_f^*$, which is asymptotically stable; the EE - no control equilibrium turns unstable. As in the *Selective seed pooling* scenario, condition D.4 can be interpreted in terms of a comparison between clean seed cost in a C-field (cN) and disease cost in an F-field at EE - no control equilibrium ($\delta g I_f^*$).

Finally, when $\mathcal{R}_0 < 1$, there are only two steady states, the DFE - no control and the DFE - full control equilibria; the former is asymptotically stable while the latter is unstable.

In contrast with the *Selective seed pooling* case, full control is never associated to an EE, and only EE - mixed control equilibria are possible. In those instances, a part of the growers adopt the C-strategy whilst the others stick to the F-strategy, taking advantage of disease dilution by the C-strategists to get reduced prevalence in their F-fields without paying the cost of control. This phenomenon is referred to as free-riding in the main text.

At the metapopulation scale, existence and stability conditions of equilibria follow from the above analysis. The DFE - no control situation corresponds to a landscape of disease free F-fields, and the DFE - full control to a landscape of (disease-free) C-fields. The EE - mixed control case results in a mosaic of disease-free C-fields and F-fields with $I_{f,m}^*$ disease prevalence, in a proportion p_m^* that varies with CS cost c, percentage loss due to disease δ and disease transmission characteristics h and ν.

The different regimes of asymptotic dynamics are illustrated with respect to clean seed cost c on Figure 2 (right column) and with respect to horizontal reproduction factor $h = e^{\beta N \tau}$ on Figure 3 (right column).

E DISEASE PROFILE AND CLEAN SEED BASED CONTROL (SELECTIVE POOLING)

Figure 7 illustrate how diseases characteristics, as captured by transmission parameters h and ν, shape growers' adoption of clean seed and landscape disease prevalence. Below the bifurcation defined by Eq. (11), no grower uses clean seed while above that threshold, all the growers are using clean seeds (Fig. 7a.). The consequence on prevalence at the landscape scale is complete control of the disease above the bifurcation condition, as well as when $\mathcal{R}_0 < 1$. The disease is able to persist in the band between those two conditions, and is maximal when hitting the clean seed uptake bifurcation threshold (Fig. 7b.). For medium disease transmission characteristics (e.g. $\mathcal{R}_0 = 1.4$), the diseases that efficiently transmit to the seed at the cost of lower in-season transmission are better controlled than those with high in-season replication and low transmission to the seed (Fig. 7b.).

F INTERACTIONS WITH OTHER DISEASE CONTROL METHODS

Figure 5 illustrates the counterintuitive effect of an additional control method through a bifurcation diagram with the disease control efficacy ω as the bifurcation parameter. The effect of the additional control method is to reduce plant-to-plant disease transmission from β to $(1 - \omega)\beta$. As ω increases from 0, clean seed uptake at equilibrium decreases and disease prevalence at the landscape scale increases. At some point the bifurcation governing

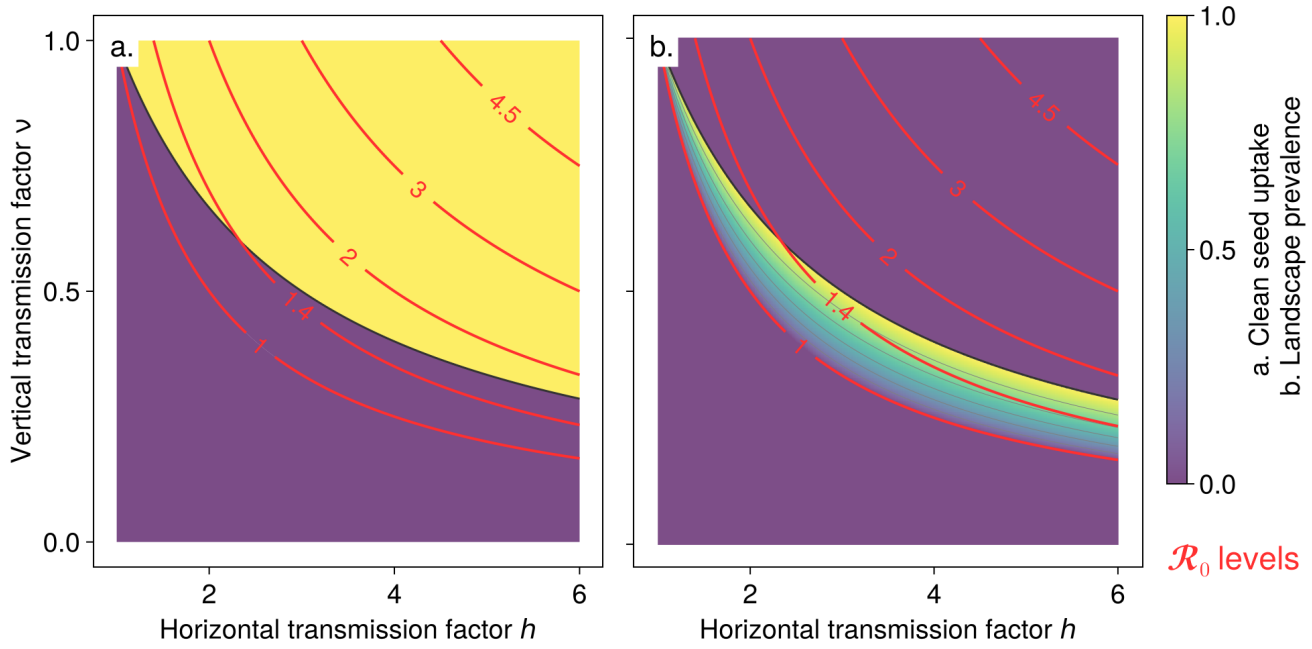

Figure 7: Impact of horizontal and vertical transmission on clean seed uptake and landscape prevalence (Selective seed pooling). Heatmaps represent the stable equilibrium value of the proportion of CS-fields and the resulting disease landscape prevalence. The thick black line indicates the bifurcation triggering CS use (UT). Thin grey lines are level curves of the variable associated to the heatmap. Dark red lines indicate constant season-to-season $\mathcal{R}_0$ levels.

clean seed uptake is crossed, clean seed is no longer used, and disease control relies solely on the additional control method. The expected negative correlation between ω and F-field and landscape disease prevalences shows up. As ω increases further, the season-to-season reproduction number of the disease drops below 1, and the disease is wiped out from F-fields and the landscape alike due to the dominance of the alternative control method.

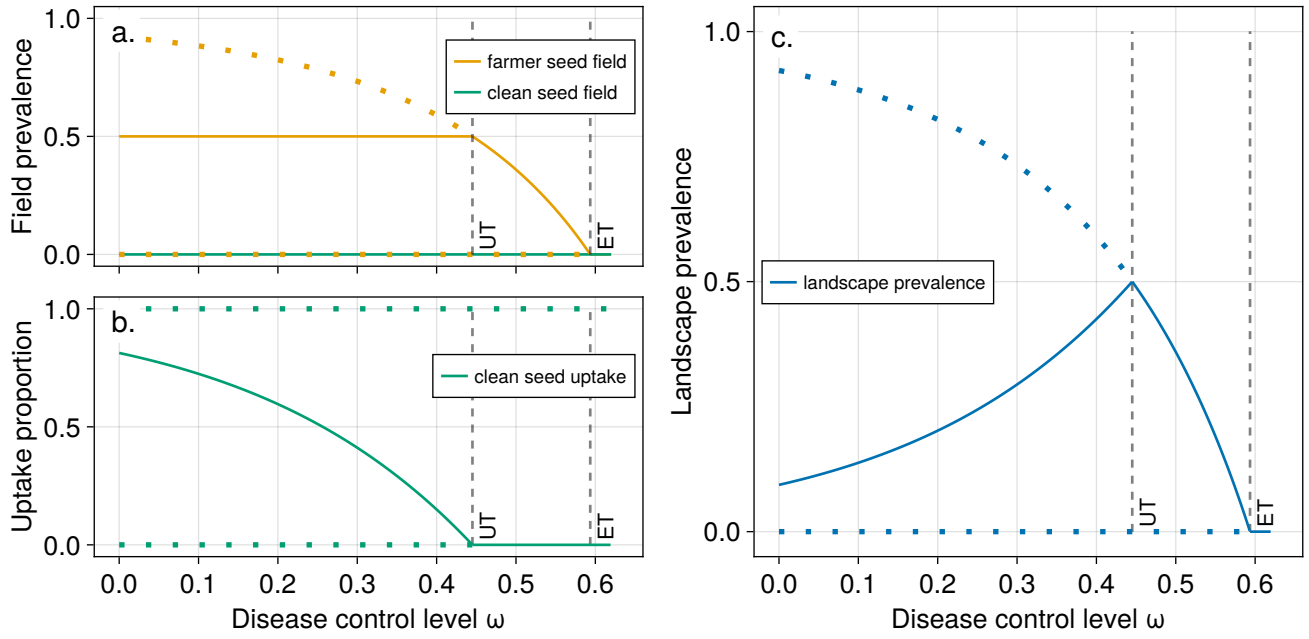

Figure 8: Bifurcation diagram with respect to disease control level (Landscape seed pooling). Equilibria for the *Landscape seed pooling* scenario as a function of the level of disease control ω. Stable equilibria are plotted with plain lines, unstable ones with dotted lines. The gray dashed vertical lines correspond to bifurcation thresholds (Epidemic Threshold - ET, and clean seed Uptake Threshold - UT).

G COMPARISON WITH CENTRALIZED OPTIMIZATION

In this section, we compare the behavioural epidemiology model with centralized optimization benchmarks at steady state (in the case $\mathcal{R}_0 > 1$). The optimized objective can be either (i) minimizing disease level at landscape scale (epidemiological optimum), or (ii) maximizing landscape-level payoff (bioeconomic optimum). More precisely, we assume that the proportion of clean seed uptake among growers is time-invariant and treat it as a control variable, to optimize the considered quantity.

On the one hand, disease level at landscape scale has already been determined in Appendix A. At equilibrium, it reads:

$$I_\ell^* = pnI_c^* + (1-p)nI_f^* = (1-p)nI_f^*.$$

On the other hand, landscape-level payoff at equilibrium $\Pi_e^* II = np\Pi_c^* + n(1-p)\Pi_f^*$ can be computed from Equations (B.1) and (4) as:

$$\Pi_\ell^* = pn(g-c)N + (1-p)n(gN - \delta g I_f^*).$$

Selective pooling scenario

In this scenario, disease level in F-fields at equilibrium is independent of clean seed uptake p (Eq. C.3). Thus:

$$I_\ell^* = (1-p)n\frac{\nu h - 1}{\nu(h-1)},$$

so that the epidemiological optimum corresponds to $p = 1$, with $I_l^* = 0$.

Regarding the bioeconomic optimum, one gets:

$$\Pi_\ell^* = n\left[g\left(1 - \delta\frac{\nu h - 1}{\nu(h-1)}\right) + p\left(\delta g\frac{\nu h - 1}{\nu(h-1)} - c\right)\right]N,$$

so that if $c < \delta g\frac{\nu h-1}{\nu(h-1)}$, the landscape-level payoff Π_l^* is maximal when $p = 1$. Conversely, if $c > \delta g\frac{\nu h-1}{\nu(h-1)}$, Π_l^* is maximal when $p = 0$. These are the same results as those predicted at equilibrium in the behavioural epidemiology model (Appendix C), with (optimal) landscape payoff corresponding to:

$$\Pi_{\ell,o}^* = \begin{cases} n(g-c)N, & \text{when } c < \delta g\frac{\nu h-1}{\nu(h-1)}, \\ ng\left(1 - \delta\frac{\nu h-1}{\nu(h-1)}\right)N, & \text{when } c > \delta g\frac{\nu h-1}{\nu(h-1)}. \end{cases} \tag{G.1}$$

Landscape pooling scenario

In that scenario, disease level in F-fields at equilibrium can be computed from the first equation in (D.1) with $p_k = p$, a constant. One gets for the non-trivial equilibrium:

$$I_f^* = \frac{\nu h(1-p) - 1}{\nu(h-1)(1-p)}N,$$

which is positive only when $\mathcal{R}_0 = \nu h > 1$ and $p < 1 - \frac{1}{\mathcal{R}_0} = p_o$. When $p \geq p_o$, disease dilution in the seed pool is large enough to fully suppress the disease and $I_f^* = 0$.

At landscape scale, this yields:

$$I_\ell^* = \begin{cases} n\,\dfrac{\nu h(1-p)-1}{\nu(h-1)}\,N, & \text{if } p < p_o, \\ 0, & \text{if } p \geq p_o, \end{cases}$$

so that the epidemiological optimum is reached for any proportion of clean seed users p larger than p_o, with $I_l^* = 0$ (akin to herd immunity in classical epidemiology).

The landscape-level payoff can be computed similarly; we get:

$$\Pi_\ell^* = \begin{cases} n\left[g\left(1-\delta\dfrac{\nu h-1}{\nu(h-1)}\right)+p\left(\delta g\dfrac{h}{h-1}-c\right)\right]N, & \text{if } p < p_o, \\ n(g-pc)N, & \text{if } p \geq p_o, \end{cases}$$

On the one hand, Π_ℓ^* is decreasing in p for $p \geq p_0$. On the other hand, the condition:

$$c < \delta g \frac{h}{h-1}, \tag{G.2}$$

determines if Π_ℓ^* is increasing or decreasing in p for $p < p_o$. Consequently, if Eq. (G.2) holds true, Π_l^* is maximized for $p = p_o$, otherwise Π_ℓ^* is maximized for $p = 0$. The optimal payoff in that case is then:

$$\Pi_{\ell,o}^* = \begin{cases} n(g-p_o c)N, & \text{when } c < \delta g \frac{h}{h-1}, \\ ng\left(1-\delta\frac{\nu h-1}{\nu(h-1)}\right)N, & \text{when } c > \delta g \frac{h}{h-1}, \end{cases}$$

which differs from the behavioural epidemiology prediction for the *Landscape pooling* scenario that reduces to Eq. (G.1).

In fact, bioeconomic optimal clean seed uptake generally differs from the equilibrium of the behavioural epidemiology model. Indeed $p_o > p_m^*$ when clean seed cost is positive (Eq. D.3). Furthermore, it can easily be shown that the cost threshold defined in Equation (G.2) is always larger than the cost threshold defined in Equation (10) for the behavioural model. When c lies between these two thresholds, the behavioural model predicts growers would abandon the strategy entirely while the bioeconomic optimum would still be a proportion of clean seed uptake $p = p_o$. In fact, the bioeconomic optimum always dictates a larger clean seed uptake to make the most of disease dilution in the seed pool at the benefit of disease control in F-fields. By doing so, landscape payoff can be maximized, but clean seed users are clearly disadvantaged compared to farmer seed users.

Only when $c = 0$, or when the bioeconomic optimum is to not use clean seeds at all, do both the behavioural epidemiology prediction and the bioeconomic optimum coincide. With respect to disease control, when clean seed cost c is low, i.e. when Eq. (G.2) holds, the bioeconomic optimum $p = p_o$ is also epidemiologically optimal. But when c is higher, the bioeconomic optimum $p = 0$ is no longer the best from the epidemiological perspective. These results are summarized in Figure 6.

H INCENTIVES FOR CONTRIBUTION TO THE FARMER SEED POOL

In Figure 9, we directly compare the *Selective seed pooling* scenario without subsidy, with a *subsidized Landscape seed pooling* scenario in which clean seed users get a discount on clean seeds for their contribution to disease dilution in the farmer seed pool. This amounts to replace clean seed cost c by $(1-\sigma)c$, with σ the reduction proportion, in the *Landscape pooling* scenario. This does not change any of the mathematical developments performed in Appendix D, albeit quantitatively lowering the threshold for clean seed uptake (Figure 9b.). The comparison between these two scenarios reveals that, at landscape scale, the disease peaks lower, and for lower disease transmission capacities, in the *subsidized Landscape pooling* scenario. Nevertheless, as soon as the clean seed uptake threshold is crossed in the *Selective pooling* scenario, the disease gets fully controlled so that the scenario regains the advantage over the other. Overall, the *subsidized Landscape pooling* scenario performs equally to or worse than the *Selective pooling* scenario over most of the range of in-season transmission capacities. The former performs better than the latter only in the narrow interval between the two clean seed uptake bifurcation thresholds (Figure 9). This general superiority of the *Selective pooling* scenario illustrates, despite the subsidy, the complex interplay between clean seed uptake as predicted by behavioural dynamics and realized disease control at landscape scale. Similar results are obtained with respect to the seed transmission capacities ν (not shown).

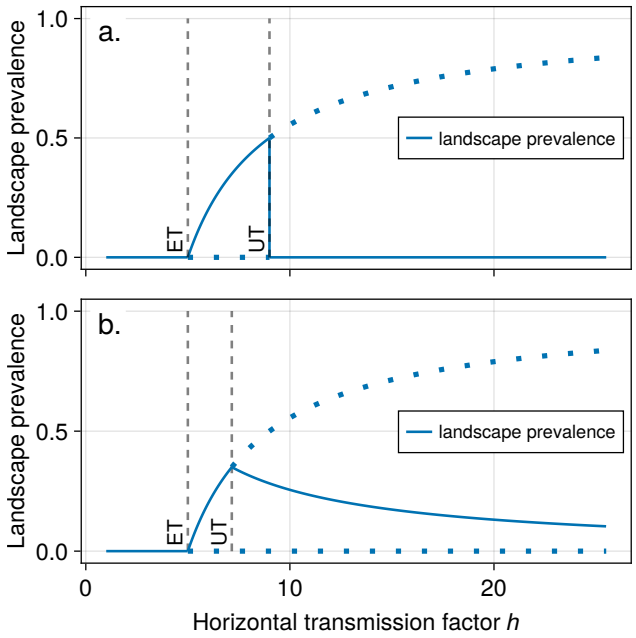

Figure 9: Landscape prevalence as a function of the horizontal disease transmission factor when the C-strategy is subsidized to contribute to farmer seed pools. Comparison between unsubsidized *Selective* (panel a.) and subsidized *Landscape* (panel b.) seed pooling scenarios when a 30% reduction is applied on clean seed cost for the *Landscape* pooling scenario. Stable equilibria are plotted with plain lines, unstable ones with dotted lines. The gray dashed vertical lines correspond to bifurcation thresholds (Epidemic Threshold - ET, and clean seed Uptake Threshold - UT).